

CHALMERS



Analysis of Progressive Landslides

A review of the simplified calculation model

Master of Science Thesis in the Master's Programme Geo and Water Engineering

LIW REHNSTRÖM

Department of Civil and Environmental Engineering
Division of Geo Engineering
Geotechnical Engineering Research Group
CHALMERS UNIVERSITY OF TECHNOLOGY
Göteborg, Sweden 2013
Master's Thesis 2013:5

MASTER'S THESIS 2013:5

Analysis of Progressive Landslides

A review of the simplified calculation model

Master of Science Thesis in the Master's Programme Geo and Water Engineering

LIW REHNSTRÖM

Department of Civil and Environmental Engineering

Division of Geo Engineering

Geotechnical Engineering Research Group

CHALMERS UNIVERSITY OF TECHNOLOGY

Göteborg, Sweden 2013

Analysis of Progressive Landslides
A review of the simplified calculation model
Master of Science Thesis in the Master's Programme Geo and Water Engineering
LIW REHNSTRÖM

© LIW REHNSTRÖM, 2013

Examensarbete / Institutionen för bygg- och miljöteknik,
Chalmers tekniska högskola 2013:5

Department of Civil and Environmental Engineering
Division of Geo Engineering
Geotechnical Engineering Research Group
Chalmers University of Technology
SE-412 96 Göteborg
Sweden
Telephone: + 46 (0)31-772 1000

Chalmers Reproservice
Göteborg, Sweden 2013

Analysis of Progressive Landslides
A review of the simplified calculation model

Master of Science Thesis in the Master's Programme Geo and Water Engineering

LIW REHNSTRÖM

Department of Civil and Environmental Engineering

Division of Geo Engineering

Geotechnical Engineering Research Group

Chalmers University of Technology

ABSTRACT

This master thesis is a study of the analysis method for progressive landslides in long natural slopes as developed by Stig Bernander. The progressive failure analysis emphasizes the importance of considering the effect of the deformations formed in the shear zone of the slope. The method also incorporates the deformation-softening properties of soft Scandinavian clay.

The work associated with the thesis has been focused on Bernander's simplified calculation method using a finite difference model in Microsoft Excel. With the intention of reducing the calculation time and making the results more accessible, conditions for applying relevant equations were implemented along with the recording of macro functions. In accordance with the purpose of increasing the transparency of the calculation process and making it easy to follow, the process has been simplified as much as possible, any computations with little effect on the end result has been omitted. The principal intension with the simplified model is to give a quick indication of risk. The short calculation time allows for an easy variation of parameters that can be used in a statistical analysis.

In addition to the attempt of making the simplified model easier to use, further opportunities for development were also investigated. As a step in this direction a simple variation of soil density by depth was added to the model. The performed sensitivity analysis revealed that the calculation results can be affected by the number of calculation steps, this dependence might be beneficial to investigate further. Previous studies by Bernander showed that the geometry of the slope is one of the most influential parameters; future development in this regard might be valuable. A better determination of the deformation softening parameters is also recommended in order to improve the reliability of the calculation model.

As a consequence of applying the deformation-softening concept rather than a fixed value for the shear strength, the traditional factors of safety does not apply to this model. Instead, a ratio between the critical deformation and the deformation caused by the applied disturbance is suggested for this type of brittle system where the residual strength is less than the in situ stress.

Key words:

Progressive landslides, Slope stability, Clay, Deformation softening, Finite difference method, Brittle failure in clay

Analys av progressiva skred
En bearbetning av den förenklade beräkningsmodellen
Examensarbete inom Geo and Water Engineering
LIW REHNSTRÖM
Institutionen för bygg- och miljöteknik
Avdelningen för Geologi och Geoteknik
Forskargruppen Geoteknik
Chalmers tekniska högskola

SAMMANFATTNING

Den här masteruppsatsen är en studie av den metodik för progressiva skred som har framarbetats av Stig Bernander. Metodiken lämpar sig för analys av långa flacka slänter med mjuk skandinavisk lera. Lerans deformationer och dess karakteristiska deformationsmjuknande egenskap är två av de aspekter som betonas särskilt i analysmetoden.

Tyngdpunkten för uppsatsen ligger på en förenklad analysmetod där finita differensberäkningar utförs i Microsoft Excel. En omarbetning av Bernanders befintliga beräkningsark i Excel har utförts med det huvudsakliga syftet att underlätta arbetet för användaren.

Parallellt med förenklingsarbetet har även fortsatta utvecklingsmöjligheter undersökts. Som stöd för denna utvärdering har en grundläggande sensitivitetsanalys genomförts. Beräkningsresultaten har även verifierats mot Bernanders tidigare publicerade resultat.

Sensitivitetsanalysen visar att modellen kan vara känslig för antalet beräkningssteg och hur storleken på beräkningsintervallen fördelas, detta är något som bör studeras vidare. Andra möjliga områden för vidareutveckling av den förenklade beräkningsmodellen är en anpassning av släntens geometri så att den bättre återknyter till faktiska förhållanden, samt att utreda parametrarna för deformationsmjuknande. Ett tillägg till modellen som har införts är en förändring av variabeln för lerans densitet så att denna parameter ökar med djupet.

I och med att skjuvhållfastheten för leran baseras på principen för deformationsmjuknande går den traditionellt använda definitionen av säkerhetsfaktorn inte att tillämpa på beräkningar baserade på modellen för progressiva skred. En kvot mellan kritiska och beräknade deformationer kan istället förordas.

Nyckelord: Progressiva skred, Släntstabilitet, Lera, Deformationsmjuknande, Sprött brott, Skandinavisk mjuk lera, Finita differenser

Contents

ABSTRACT	I
SAMMANFATTNING	II
CONTENTS	III
PREFACE	V
NOTATIONS	VI
1 INTRODUCTION	1
1.1 Background	1
1.2 Aim	1
1.3 Method	1
1.4 Delimitations	2
2 LITERATURE STUDY	3
2.1 Mechanisms behind a slope failure	3
2.1.1 Material properties for soft Scandinavian clay	4
2.2 Description of traditional analysis methods	5
3 METHODOLOGY FOR ANALYSIS OF PROGRESSIVE LANDSLIDES	6
3.1 Definition of progressive slides	6
3.2 Description of the failure process	6
3.3 Basic principles	7
4 CALCULATION METHOD IN PROGRESSIVE FAILURE ANALYSIS	10
4.1 General outline and basic assumptions	10
4.2 Calculations using the Excel spreadsheet	12
4.2.1 Verification with previous examples by Bernander	17
4.2.2 Calculations for a new slope example	21
4.2.3 Calculation Results	24
4.2.4 Sensitivity Analysis	25
5 DISCUSSION	28
5.1 Comments on the model and calculation method	28
5.2 Discussion of relevant safety factors	29
6 CONCLUSIONS	30
7 REFERENCES	31

APPENDIX 1. COMPILATION OF EQUATIONS IN EXCEL

APPENDIX 2. TRANSLATION OF EQUATION NUMBERING

APPENDIX 3. INPUT AND RESULTS FROM VERIFICATIONS WITH
PREVIOUS VERSIONS OF SPREADSHEETS DEVELOPED BY BERNANDER

APPENDIX 4. RESULTS FROM SENSITIVITY ANALYSIS

Preface

This thesis is an attempt to summarise parts of the extensive work by Stig Bernander on the subject of progressive landslides. His methodology has been developed over the course of about 40 years and has so far resulted in a number of publications and software applications. The intension of this thesis has been to give an introduction to the subject and attempt a development of the existing Microsoft Excel spreadsheets by Bernander in order to simplify and facilitate further development. The work has been conducted in collaboration with Skanska Sverige AB, under the guidance of Anders Kullingsjö. I owe him many thanks for his determination and support throughout the project.

I would also like to thank Stig Bernander for the time and effort he took in explaining some of the aspects of the theory. His dedication and knowledge on the subject was a true inspiration.

Göteborg December 2012

Liw Rehnström

Notations

Roman letters

C	Compatibility criterion between deformation and displacements
c_{factor}	Factor for increasing or decreasing peak shear strength according to influence from loading time
c_{lab}	Peak shear resistance measured in laboratory
c_R	Residual shear resistance
c	Peak shear resistance
c_s	Shear resistance at surface
d_{gain}	Additional density gain with depth
d_{start}	Start value of density variation with depth as $\rho = d_{start} + z * d_{gain}$
E	Elastic modulus
G	Modulus in shear
H	Height from slip surface to surface
L_{crit}	Limit length where shear resistance can be mobilised
N_{crit}	Maximum value of additional force
x	Coordinate for length starting at foot of slope
q	Critical load [kN/m ²]
z	Coordinate for depth
S_t	Sensitivity of clay

Greek letters

$\tau_0 (z=0)$	Shear stress in situ at slip surface
τ_0	Shear stress in situ
$\tau + \Delta\tau$	Additional shear stress
τ_{max}	Shear stress
τ_{el}	Shear stress at elastic limit
ρ	Density of material
γ_f	Deviator strain at peak shear resistance
γ_{el}	Deviator strain at elastic limit
$\delta(\tau)$	Displacement due to shear deformation
$\delta(N)$	Displacement due to deformation generated by force N

δ_{slip}	Deformation at slip surface in relation to sub-ground
δc_R	Deformation in slip surface at residual strength
δ	Deformation
α	Coefficient defining elevation for earth pressure resultant
$\Delta\tau$	Differential in shear resistance
Δz	Differential in z coordinate
Δx	Differential in x coordinate
ΔN	Differential in pressure
ν	Poisson's ratio

1 Introduction

This chapter provides a background to the thesis along with the intended purpose and delimitations. The intention and scope of the project will be explained and the method outlined.

1.1 Background

Why and how a seemingly stable slope suddenly can collapse, leaving the landscape so dramatically changed, is perhaps a question of natural curiosity and fascination. Human interaction with the environment leaves traces; new constructions and infrastructure require more land use than ever before. Both urban and rural areas become more densely developed and not only the risk, but also the consequences, of a natural disaster like a landslide, increase with human presence and activity. As the stakes are raised, reliable methods for analysis are required to target and develop dependable solutions for preventive action.

Ever-changing conditions and circumstances not entirely known make the subject of slope stability extremely complex. The analysis requires both simplifications and assumptions. Making the problem manageable without compromising the accuracy of the results is a difficult task. Over the years, numerous models and calculation methods have been developed and as always with a theory - the discrepancy between model and actual conditions is a subject for debate. A number of improvements have been proposed, rejected or implemented. One of the proposed approaches to stability problems in long natural slopes with soft Scandinavian clay is the method of progressive failure analysis developed by Stig Bernander. Instead of the more traditional method based upon limit equilibrium, he proposes a numerical finite difference model that takes the deformation properties into consideration.

1.2 Aim

The purpose of this thesis is to:

- Give a description of the analysis method for downhill progressive failure developed by Stig Bernander.
- Illustrate the calculation process by using a simplified example in Excel, as a development of previous spreadsheets by Stig Bernander.
- Perform an elementary sensitivity analysis on the spreadsheet calculations.
- Discuss relevant safety factors for progressive failure analysis.

1.3 Method

As an introduction, a literature study was performed on the subject of slope stability. A brief summary of this study is included in Chapter 2 of the thesis, along with a mention of the most commonly used method for slope stability problems in western Sweden today. This provides a background and a contrast to the focus of this thesis; the analysis method for progressive slides in long natural slopes.

The theory behind the method developed by Stig Bernander is outlined in Chapter 3, where definitions, processes and basic principles are conveyed. The analysis method is described further in Chapter 4, where the calculations in the Excel software are presented. Previous spreadsheets by Bernander have been developed into a new version. The purpose of this has been to simplify the calculation process and

investigate possibilities for further developments. The new version is verified against previous examples published by Stig Bernander.

Calculations for a simplified model of an infinite slope have been carried out and the variations of parameters are studied in an elementary sensitivity analysis. The input values for the different variables in the calculations have been chosen to emulate clay slopes in typical conditions in south western Sweden. Simplifications have been made in order to give a better understanding of the basic principles of the method, as the calculation time is reduced and complexity, that was deemed unnecessary, is omitted.

The results of the calculations are analysed in Chapter 5. The advantages and disadvantages of the method are discussed as well as possible further developments and relevant safety factors.

1.4 Delimitations

The scope of this thesis is to give a description of Stig Bernander's method for evaluating stability for long natural slopes in soft Scandinavian clay. It is not however a full account of the methodology, for more elaboration and detail the reader is referred to the works of Stig Bernander.

The method of analysis referred to, is primarily dedicated to determining safety for long natural shallow slopes in normally consolidated soft clay, with properties typical for the south western part of Sweden. The slope example used in the calculations is chosen with consideration to this limitation. It models a very simplified set of conditions for a slope as the purpose is to convey the principles of the method and provide an initial risk evaluation, rather than a full scale in-depth analysis.

2 Literature study

A short summary of the conducted literature study is given in this chapter. A brief description of the soil properties and the analysis methods used for soft Scandinavian clay serve as a background and a contrast to the method of progressive failure analysis.

2.1 Mechanisms behind a slope failure

There are a number of factors known to affect the stability of a slope. Some of the more important variables, according to the Swedish Geotechnical Institute (2012) are:

- stratigraphy; soil types, properties and constitution,
- geometry of the slope,
- ground- and surface water conditions,
- rate of additional loading.

The balance of the slope can be disrupted if the load is increased, the counterweight is reduced or if the soil loses strength (Swedish Geotechnical Institute, 2012). As the driving forces in the active zone increase and the stabilising forces in the passive zone are reduced, a slip surface forms as illustrated in Figure 2.1. If the destabilising process continues a slide of the soil mass above the slip surface will eventually occur.

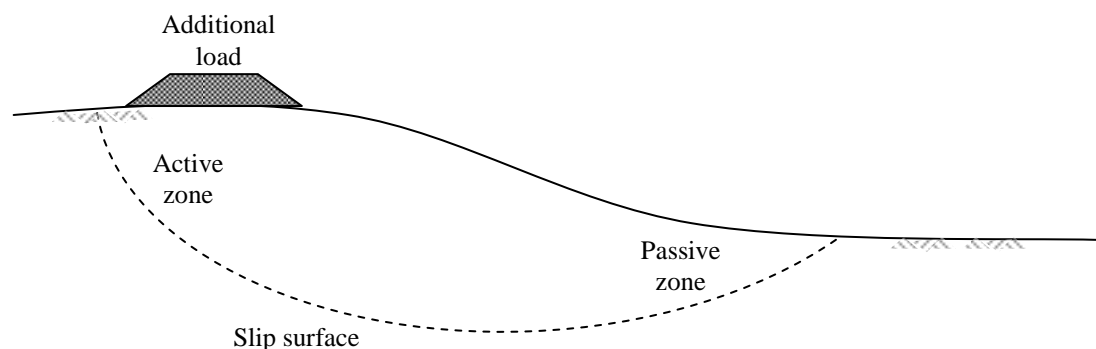


Figure 2.1. Simplified illustration of a slope with formation of a slip surface.

As part of the risk evaluation a total safety factor, denoted F , for the slope can be calculated as:

$$F = \frac{\bar{\tau}_f}{\bar{\tau}_{mob}}$$

Where $\bar{\tau}_f$ is the average shear strength along a designated slip surface and $\bar{\tau}_{mob}$ is the average mobilised shear resistance (Royal Swedish Academy of Engineering Sciences: Commission on Slope Stability, 1995). Values just above 1 indicate a substantial risk of slope failure. This total safety factor is foremost applicable to problems with already existing constructions and natural slopes. For cases where the safety of new developments are assessed, the method of partial coefficients is recommended since the implementation of European standards (IEG, 2010, p.3). For this method each critical variable is assigned a separate factor of safety instead of applying a factor of safety on the completed calculation.

It is always important to keep in mind that the total risk factor does not take into consideration the consequences of a failure. Guideline values of the risk factor are divided into categories according to the range of the investigation and the magnitude of the consequences (IEG, 2010, pp.10-15). For a thorough in-depth investigation where the consequences of a failure are predicted as minor, a lower factor of safety can be tolerated. As more investigations are made, the range which the parameters vary within becomes narrower. With less uncertainties connected to the variables, a lower factor of safety is sufficient to keep the result on the safe side.

2.1.1 Material properties for soft Scandinavian clay

The soft Scandinavian clay was deposited under marine conditions. As precipitation and groundwater slowly filter through the soil layers, the salt crystals imbedded in the clay formation are dissolved. As a consequence of this continuous leaching the clay structure becomes more open and unstable (Gylland, Nordal, Jostad, & Mehli, 2011, p. 576). In conditions where artesian ground water is present, i.e. upwards flow of water, the leaching increase substantially. As a result of the leaching process, the clay can become very sensitive to movements and vibration. The sensitivity of clay, denoted S_t , is measured as the quota between a stirred and an undisturbed undrained sample. Values of S_t above 50 indicate the presence of so called quick clay. An undrained shear strength below 0,4 kPa in a stirred sample is also required (Larsson, 2008, p. 23).

The properties of soft Scandinavian clay are markedly anisotropic and evaluations of laboratory tests show a typical strain softening behaviour post-peak (Andresen, 2002, p. 1). Figure 2.2 illustrates how the shear strength decreases with additional load after the initial elastic phase and peak value.

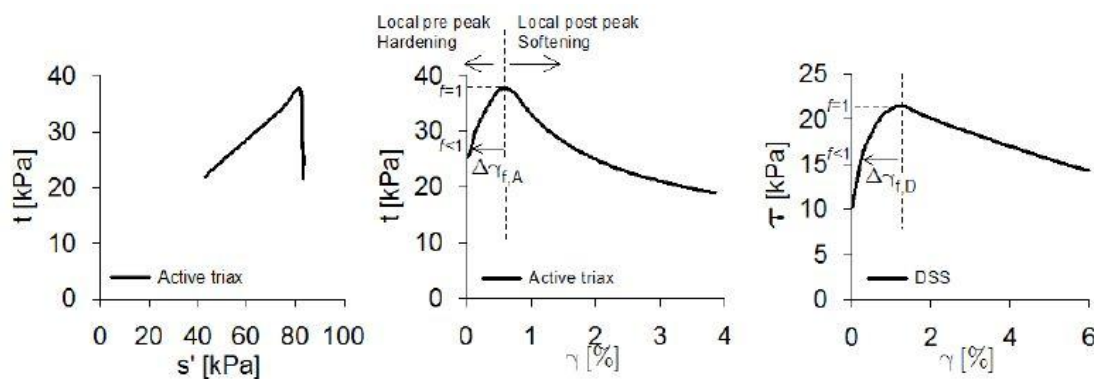


Figure 2.2. Response from triaxial compression and direct shear stress tests on Ellingsrud Clay (adapted by Gylland, Nordal, Jostad, & Mehli (2001) after Lacasse, Berre & Lefebvre (1985)).

The typical normally consolidated clay in the Gothenburg region has an average peak value for shear strength of 13-15 kPa down to a level of approximately -10 m where it gains about 1,5 kPa/m (Sällfors, 1994). If the residual shear strength, after reaching a peak value, goes below the in situ value, the slope failure is of a brittle character. Residual values approaching the peak value will give a more ductile failure process. (Bernander, 2011, pp. 160-161)

2.2 Description of traditional analysis methods

Traditionally, the most common method for slope stability calculations relies on limit equilibrium. There are a number of different computer software programmes available for calculations according to this method. Over the years the programmes have been developed to handle a number of applications in stability problems, making allowances for shifting soil stratigraphy, complex slope geometry as well as changing pore-water pressure, load conditions and reinforcements (GEO-SLOPE International Ltd, 2008, p. 7). One of the dominating software programs used in Sweden is SLOPE/W. The programme divides the soil mass above the slip surface into a number of vertical slices and calculates a mutual safety factor for all the slices using limit equilibrium. Figure 2.3 illustrates how the calculated local factor of safety differs throughout the slope for the finite element method (F.E.), whereas the limit equilibrium method (L.E.) shows no variation. The global factors of safety for the two methods are the same, but the finite element method indicates that the upper part of the slope has a local safety factor that is significantly lower than the average calculated by the limit equilibrium method.

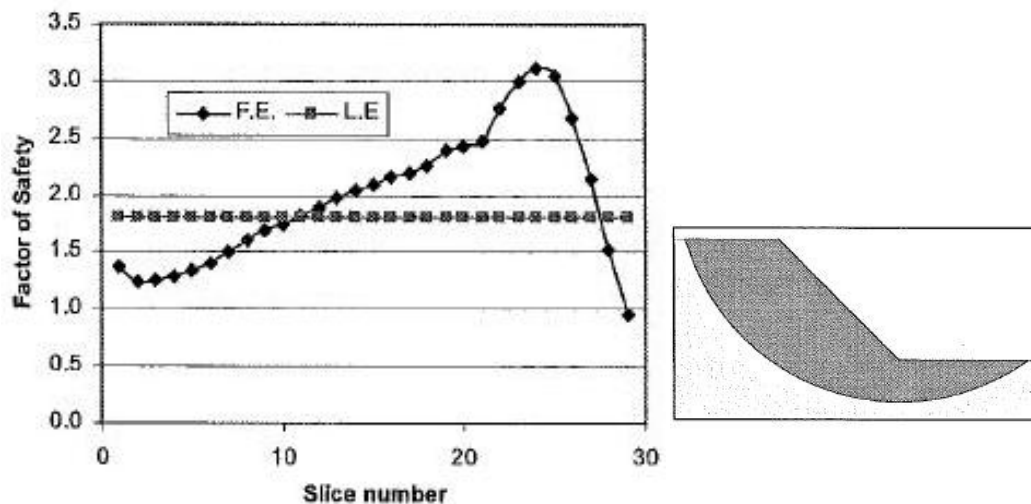


Figure 2.3. Factor of safety for Finite Element (F.E.) and Limit Equilibrium (L.E.) calculations on a deep slip surface. (GEO-SLOPE International Ltd, 2008, p. 74)

Within the limit equilibrium theory there are a number of methods to choose from; Spencer, Morgenstern-Price and Janbu Generalised are some of the most common that solve for both forces and moment equilibrium (GEO-SLOPE International Ltd, 2008, p. 10). Most of these variations give approximately the same result. The consistency of results does however not necessarily reflect on the applicability of the model: “*Any attempt to validate the limit-equilibrium approach by comparing different limit-equilibrium solutions, without reference to a more rigorous analysis, is considered to be inconclusive.*” (Yu, Salgado, Sloan, & Kim, 1998, p. 2) Limitations of the method are pointed out: “*The missing physics in a limit equilibrium formulation is the lack of a stress-strain constitutive relationship to ensure displacement compatibility.*” (GEO-SLOPE International Ltd, 2008, p. 29) Additional software, like SIGMA/W, has been designed to work together with the traditional programs in an attempt to integrate constitutive stress-deformation properties of the soil. However, the method is principally intended for application on problems involving vertical walls and is not recommended for natural slopes (GEO-SLOPE International Ltd, 2008, p. 80).

3 Methodology for analysis of progressive landslides

This chapter describe the theory behind the method of progressive failure analysis as developed by Stig Bernander. Definitions are introduced and followed by further explanations of the different concepts in the analysis method.

3.1 Definition of progressive slides

Progressive failure in natural slopes can be divided into three categories: downhill-, uphill- (retrogressive) or laterally progressive slides. An extensive landslide can often be a combination of more than one type of failure. (Bernander, 2011, pp. 22-23)

- *Uphill progressive slides:*
An uphill- or retrogressive landslide is triggered by changed conditions or disturbance at the foot of the slope. Bernander distinguishes between three stages in retrogressive slides: Existing in situ state, Disturbance and Dynamic disintegration.
- *Laterally progressive slides:*
When the destabilising forces are transferred sideways and reach a more critical section of the slope, the slide progresses laterally.
- *Downhill progressive slides:*
This type of progressive failure is the most common of the three (Bernander, 2000, p. 15) and consequently the focus of this thesis. As the name implies, the slide starts in the upper part of the slope as a local instability that propagates downhill. The failure process is divided into two stages and six phases, more about this in the next section.

3.2 Description of the failure process

In order to describe and analyse downhill progressive slides Bernander (2011, p. 23) divides the process into different phases. This distinction between phases helps separate between different conditions governing the failure process. It helps not only understanding, but also the calculation procedure, as will be explained in Chapter 4. The six phases are:

1. Where the existing in situ conditions prevail.
2. When the disturbance is created or triggered.
3. A dynamic intermediate phase where the stress is redistributed.
4. A new state of equilibrium, transitory or permanent.
5. When the passive pressure is exceeded the final breakdown of the failure zone begins.
6. The concluding state of equilibrium.

When the additional stress, caused by the disturbance, is redistributed in phase 3, a slip surface can develop if the pressure is sufficiently high. For the upper part of the slope this tends to happen along firm bottom or where there are specific sedimentary layers (Bernander, 2008, p. 37). A difference in soil composition makes the bonds between the two layers weaker, shear strength is thus reduced, creating a more vulnerable zone.

The development of a slip surface in phase 3 is a prerequisite condition for a complete slope failure, but does not however entail a landslide. If the load is removed or the disturbance ceases, the slope can once again reach a state of equilibrium that accommodates the changed conditions. In those cases, the damaged zone of the slip surface heals when the soil consolidates.

In order to mark the difference in patterns for the processes before and after the formation of the slip surface Bernander (2011, p. 38) makes a distinction between two simultaneous stages:

- I. Before slip surface formation, phase 1-3
- II. After the slip surface is formed, phase 4-6

These two stages allow the model to include time effects that influence the shear strength and incorporate the strain-softening that govern the equations used in the analysis. The two stages can coexist in different parts of the slope so that the upper part can have a fully developed slip surface when the lower part is still in the dynamic redistribution phase. The formation of the slip surface can however not coincide with the complete collapse of the passive zone which leads to a landslide (Bernander, 2008, p. 35).

3.3 Basic principles

One of the most important issues in the progressive failure analysis, regards the deformations that develop when the pressure in the soil exceed the bearing capacity. Instead of looking at the soil volume above the slip surface as one rigid body, the method of progressive failure considers the effect of the deformations within the sliding mass of clay. As the soil at the top of the slope experience additional stress or imposed displacement, the load is redistributed and if the pressure is high enough, deformations starts to develop as illustrated in Figure 3.1. When the soil is compacted this puts further stress on the adjacent soil and deformations continue to develop, or progress, downhill. As a result of the deformations, cracks form in the upper part of the slope and if these are filled with water the tension increase further (Bernander, 2011, p. 105). The process of deformation can continue to the foot of the slope and beyond. This is a characteristic feature in progressive landslides; a large portion of the area involved in the slide is usually nearly plane.

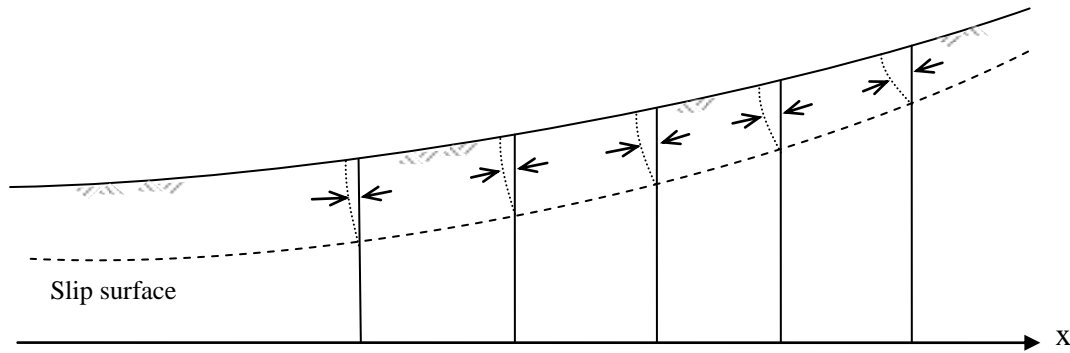


Figure 3.1. Deformation within the soil mass above the slip surface (adapted after Bernander (2011), p.181)

Development of deformations due to additional stress depends on the stress-strain relationship for the specific soil type. Traditional slope stability calculations often rely on a discrete value for the shear stress where only the peak value is used. In the progressive failure analysis the relationship between stress and strain is incorporated as a key element in the analysis. Clay as a material tends to have a softening behaviour post peak, as illustrated in Figure 3.2. After an elastic phase with shear strength up to the linear limit, denoted τ_{el} , a plastic phase begins and the peak value, c , is reached. At this point, the formation of the slip surface begins, and stage I is at an end. Stage II begins by a decline in strength (softening) until only the residual strength, c_R , remains.

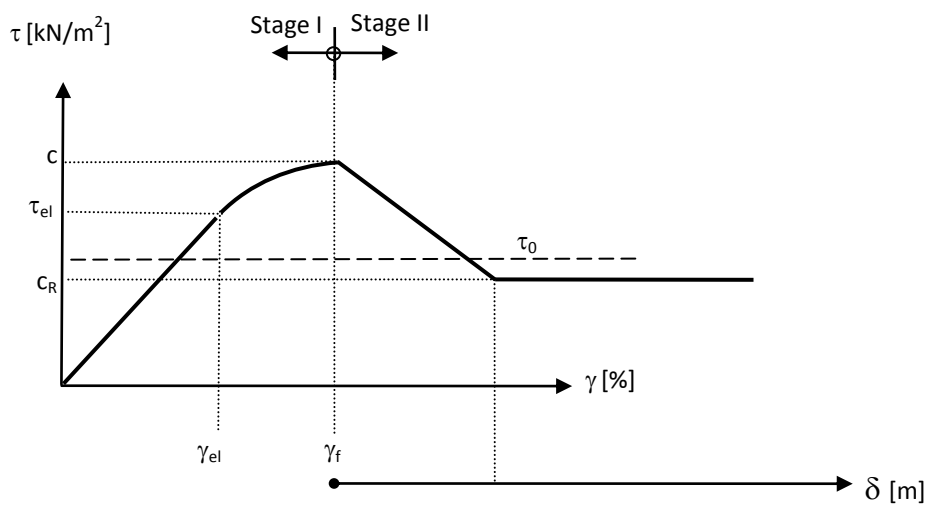


Figure 3.2. Illustration of stress-strain relationship. Notations: Stress at elastic limit (τ_{el}), peak value for shear strength (c), residual value for shear strength (c_R). Strain at elastic limit (γ_{el}), strain when peak value for shear strength (γ_f). Deformation post-peak (δ_{SR}) when residual shear strength is reached. (After Bernander (2011) p.24 & 179)

The stress-strain relationship is strictly depending on soil type, rate of loading and drainage conditions. Fast loading gives a higher peak value and a lower residual value, which implies a quick, brittle failure. The ratio between the residual value, c_R , and the peak value, c , will in this case be low. Figure 3.3 illustrates the relationship between these variables for three independent examples, with ratios ranging from of 0,4 to 1. As the difference between the peak strength and the residual strength lessen, the ratio approaches 1, and in that case the failure will be ductile. As the residual strength and peak value depends on how sensitive the clay is to loading and drainage conditions the ratio between the c_R and c , can thus be used as a measure of the sensitivity of clay. (Bernander, 2008, p. 37)

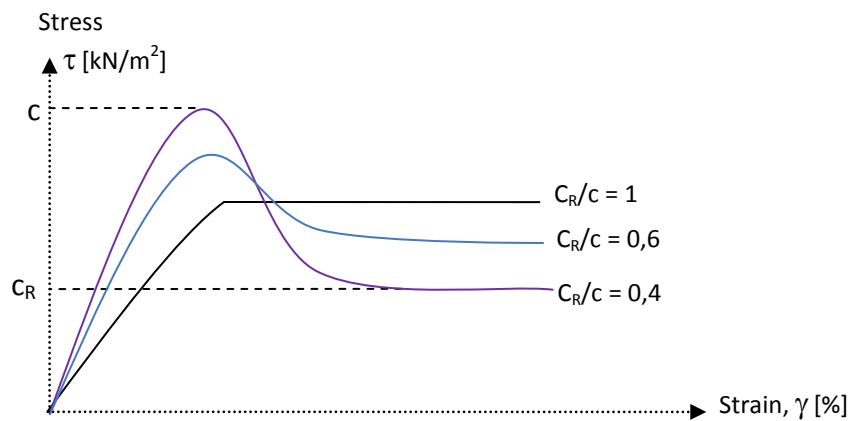


Figure 3.3. Illustration of the concept of brittleness ratio. After Bernander (2011) p. 86

How the slope reacts to changed conditions is thus a question very much regarding the influence of time. This is reflected in the distinction between stages and phases that separates the changing conditions that governs the calculation of the deformation development.

4 Calculation method in progressive failure analysis

A general description of the calculation process in progressive failure analysis is given as an introduction in this chapter along with an account of the basic assumptions made. The method is explained further by use of the Microsoft Excel Spreadsheet specifically designed for this purpose. The spreadsheet is based on previous versions by Stig Bernander and is verified against published examples of calculations. Calculations are then performed for a simplified example of a slope.

4.1 General outline and basic assumptions

The objective of the calculations is to determine the additional load capacity of the slope, represented by the component of the horizontal force denoted N_{crit} . The total length of the affected area, L_{crit} is also determined, beyond this point there is no contribution to the stabilising forces. The maximum additional load per square meter, q , as illustrated in Figure 4.1, for which the slope can maintain the status of equilibrium, can be determined by dividing the horizontal force component with the depth to the slip surface:

$$(1) \quad \text{Maximum load: } q = \frac{N_{crit}}{H}$$

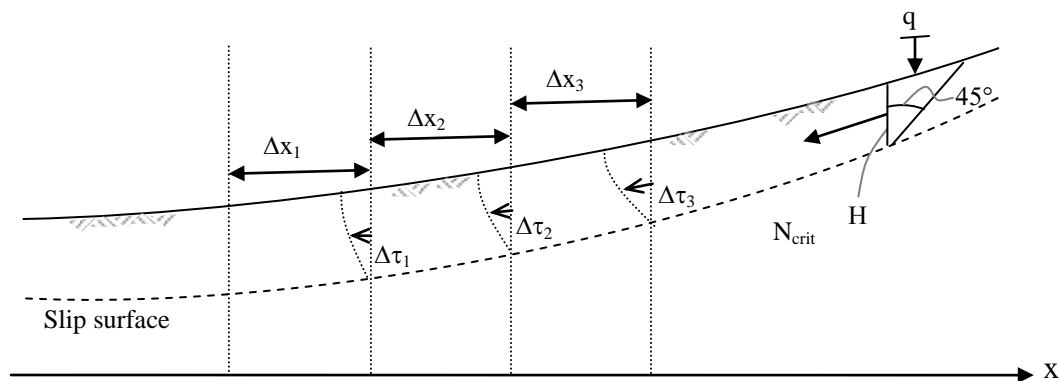


Figure 4.1. Stepwise calculation of deformation.

The starting point for the calculation is at the very foot of the slope where deformation and stress from the disturbance is presumed to be zero. With this lower boundary condition, calculation of deformations can be made stepwise upslope by adding either stress, $\Delta\tau$, or distance Δx , as illustrated in Figure 4.1. Each addition of stress corresponds with an addition in length, and vice versa. This is regulated by using a compatibility criterion denoted C , which balance the deformation due to the added shear stress, $\Sigma\delta(\tau)$, and the deformation due to added pressure, $\Sigma\delta(N)$ (Bernander, 2011, p. 42).

$$(2) \quad \text{Compatibility criterion:} \quad C = \Sigma\delta(N) - \Sigma\delta(\tau)$$

If the slope model has a variation of gradient and depth to the slip surface, it is preferable to predetermine the steps along the x -axis and regulate the difference in stress. However, if the geometry of the slope allows a simplification so that the

gradient and depth can be set as a constant, it is easier to adapt the step distance to the stress difference. (Bernander, 2011, p. 178)

The calculations in Stage I begin by determining the in situ stress, proceeding stepwise with added pressure $\Delta\tau$ and distance Δx , for each vertical segment. The process continues until the pressure reaches the level of maximum strength and the slip surface forms:

$$(3) \quad \text{Condition for completion of Stage I: } (\tau + \Delta\tau) = c$$

The second stage begins and the equations differ according to the stress-strain relationship. Deformation and slip are however still balanced by the compatibility criterion. For each calculation step upslope, the deformations are added and the procedure continues until the stress becomes equal to in situ stress again. At that point all the additional bearing capacity is used and the maximum pressure value is reached. This represents the vertical component of the critical load, N_{crit} , which is determined when the following condition is fulfilled:

$$(4) \quad \text{Determining critical load in Stage II when: } (\tau + \Delta\tau) = \tau_0$$

At this point the total length of all the steps taken is summarized, i.e. $\Sigma\Delta x$. This represents the length of the affected area, L_{crit} , where the pressure of the additional load is felt.

As previously mentioned, the shape of the stress-strain relationship can vary depending on rate of loading, draining and clay properties. As shown in Figure 4.2, Bernander use a linear dependence up to the elastic limit, τ_{el} , followed by a parabolic relationship to the power of 2 until the peak, c , is reached. In stage II, post peak, the strength is reduced according to an approximated linear dependence and a proportional deformation corresponding to the stress, δ_{cR} , is added. After the point of residual strength, slip deformation is added. The specific shape of this curve is of minor significance and can be altered. (Bernander, 2011, p. 179)

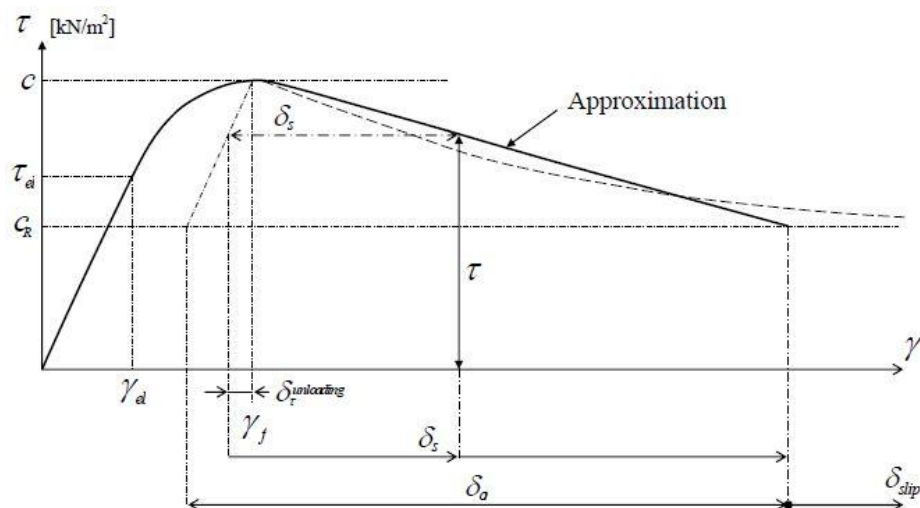


Figure 4.2. Illustration of the stress-strain relationship for clay. Notations: Stress (τ), stress at elastic limit (τ_{el}), peak value for shear strength (c), residual value for shear strength (c_R). Strain (γ), strain at elastic limit (γ_{el}), strain when peak value for shear strength (γ_f). Deformation post-peak (δ_s), deformation when residual shear strength is reached (δ_{slip}). (Bernander, 2011, p. 179)

The ratio of horizontal and vertical stress is set as constant. As the in situ conditions are determined the total stress is considered, not the effective stress (Bernander, 2011, p. 148). This is consistent with the objective to calculate the deformation with as little complication as possible.

The location of the earth pressure resultant is set at the height of 1/3 of the depth to the slip surface. This is a simplification but the impact of this parameter is low. A sensitivity analysis for this parameter has been performed by Bernander which shows that the influence of the variable on the end result is slight for normally consolidated clay (2011, p. 44).

Where in the soil profile the slip surface forms, is regarded as prerequisite input to the analysis. Determining the most dangerous placement can be the result of an assessment by the engineer and a trial-and-error process as several scenarios are compiled and analysed by calculation.

4.2 Calculations using the Excel spreadsheet

The current spreadsheet is designed for an infinite slope with constant inclination and depth to slip surface, illustrated in Figure 4.3. After the input parameters and material properties have been entered, the calculations are carried out with the help of conditional loops so that the appropriate equation is selected for each set of conditions. This limits the number of spreadsheets from the two versions previously used to only one. In order to simplify calculation the Solver tool in Excel is used for determining deformations and fulfilling the compatibility criterion. For this purpose a macro has been recorded so that users only have to click a button. One additional macro calculates the last step where the residual strength is reached. The use of Excel macros and Solver enables the user to perform a series of calculations within minutes. The easy variation of parameters is useful when a statistical analysis is performed.

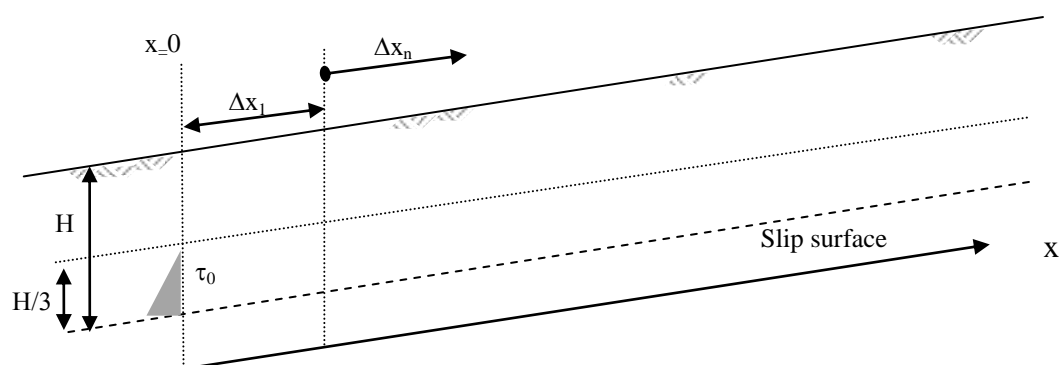


Figure 4.3. Calculation of in situ conditions.

A list of the required input variables are compiled in Table 4.1. The parameters of shear modulus, G , mean elastic modulus, E_{mean} , and strain at the elastic limit, γ_{el} , are functions of the other input variables and are calculated according to the following equations:

$$(5) \quad G = \frac{\tau_{el}}{\gamma_{el}}$$

$$(6) \quad E_{mean} = \frac{G}{c_{peak}} * 2 * (1 + \nu) \frac{(c_s * c)}{2}$$

$$(7) \quad \gamma_{el} = \frac{\gamma_f * \tau_{el}}{(2 * c_{peak} - \tau_{el})}$$

$$(8) \quad c = c_{lab} * c_{factor}$$

Table 4.1. Required input variables to the spreadsheet calculations.
(Variables marked with * are calculated.)

Shear strength at surface	c_s	kN/m ²
Peak value for shear strength evaluated in lab	c_{lab}	kN/m ²
Factor for increasing peak shear strength	c_{factor}	%
Residual value for shear strength	c_R	kN/m ²
Shear stress at elastic limit	τ_{el}	kN/m ²
Deviator strain at elastic limit *	γ_{el}	%
Deviator strain at failure limit	γ_f	%
Elastic modulus at shear *	G	-
Elastic modulus *	E_{mean}	-
Poisson's ratio	ν	-
Post peak slip at $z=0$ when c_R is reached	δ_{cR}	m
Density:	d_{start}	kN/m ²
	d_{gain}	kN/m ²
Depth to slip surface	H	m
Gradient	$\Delta y / \Delta x$	-

As previously mentioned, the calculations start off in Stage I, where the shear pressure is below the maximum value, c . The in situ value of the pressure, denoted τ_0 , at the level of the prospective slip surface ($z = 0$) is calculated as a function of soil density at the given depth, ρ , together with the depth to the slip surface, H , and inclination of slope, denoted $grad$:

$$(9) \quad \tau_{0(z=0)} = \rho(z) * H * \sin(\arctan(grad)) * g$$

Above this depth the stress, $\tau_{0(z=n)}$, declines linearly depending on the difference in depth, denoted Δz :

$$(10) \quad \tau_{0(z=n)} = \tau_{0(z=0)} * \left(\frac{1 - \Delta z}{H} \right)$$

The shear zone where the principal deformations develop, is restricted to a third of the depth down to the slip surface, as illustrated in Figure 4.3. The figure also shows how the slope is divided into horizontal segments, with the length of Δx . The stress increase by $\Delta \tau$ for every step starting with the in situ value, τ_0 , continuing to the peak value, c , which indicate the end of Stage I. In this version of the spreadsheet the number of segments in Stage I, is set to nine. This number can be changed if higher resolutions in the results are required.

Deformation of each segment is calculated using the compatibility criterion previously mentioned. This requires that the deformation caused by the shear stress, $\Sigma\delta(\tau)$, is equal to the displacement caused by the horizontal pressure, $\Sigma\delta(N)$.

The impact of the additional load on the earth pressure, ΔN , for a segment, is calculated as the difference between the additional stress and the in situ stress multiplied with the distance Δx according:

$$(11) \quad \Delta N = \left(\frac{(\tau + \Delta\tau_{(z=0)} + \tau_{(z=0)})}{2} - \tau_{0(z=0)} \right) * \Delta x$$

The added earth pressure is then summarised for each section:

$$(12) \quad \Sigma\Delta N_{(x=n+1)} = \left(\frac{(\tau + \Delta\tau_{(z=0)} + \tau_{(z=0)})}{2} - \tau_{0(z=0)} \right) * \Delta x + \Delta N_{(x=n)}$$

The total sum of displacement caused by the horizontal pressure is calculated as a function of the added pressure ΔN , length of the segment Δx , depth from surface to slip surface, H , and the average elastic modulus for the shear zone, E_{mean} :

$$(13) \quad \Sigma\delta(N) = \frac{(\Delta N_{(x=n)} + \Delta N_{(x=n+1)})}{2} * \frac{\Delta x}{E_{mean} * H}$$

How the deformation due to the additional shear pressure is calculated, depends on the stress-strain relationship. Figure 4.5 illustrates the conditions for the equations determining the deformation, $\delta(\tau)$, in Stage I. The choice of equation depends on how the starting in situ value, τ_0 relates to the elastic stress limit, τ_{el} .

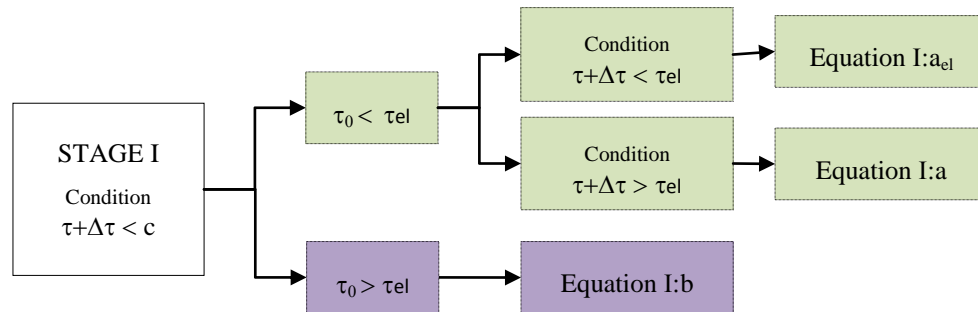


Figure 4.5. Conditions for equations in Stage I.

This dependence, for the case where the in situ stress is within the elastic region, can also be illustrated as seen in Figure 4.6. When the in situ stress exceeds the elastic limit, the equations illustrated in Figure 4.7 are used.

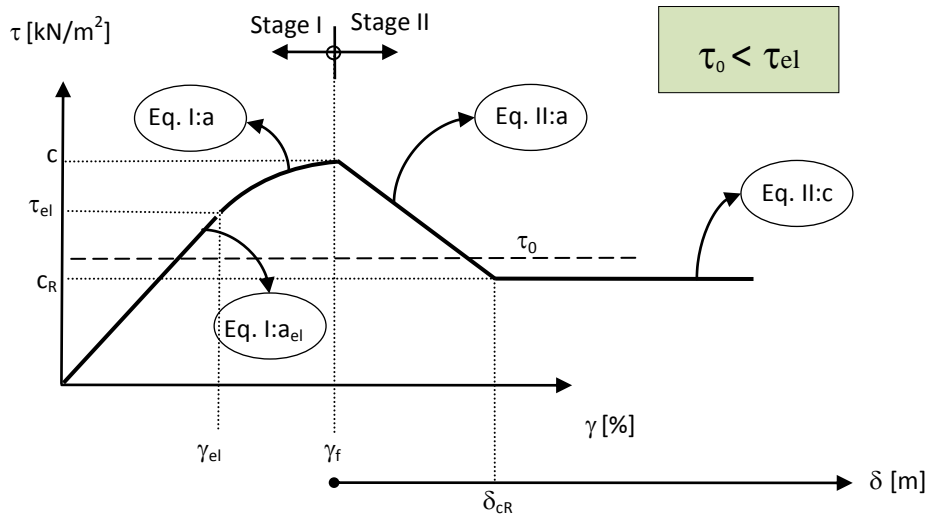


Figure 4.6. Stress-Strain relationship and equations for deformation by additional stress when in situ stress is within the elastic segment.

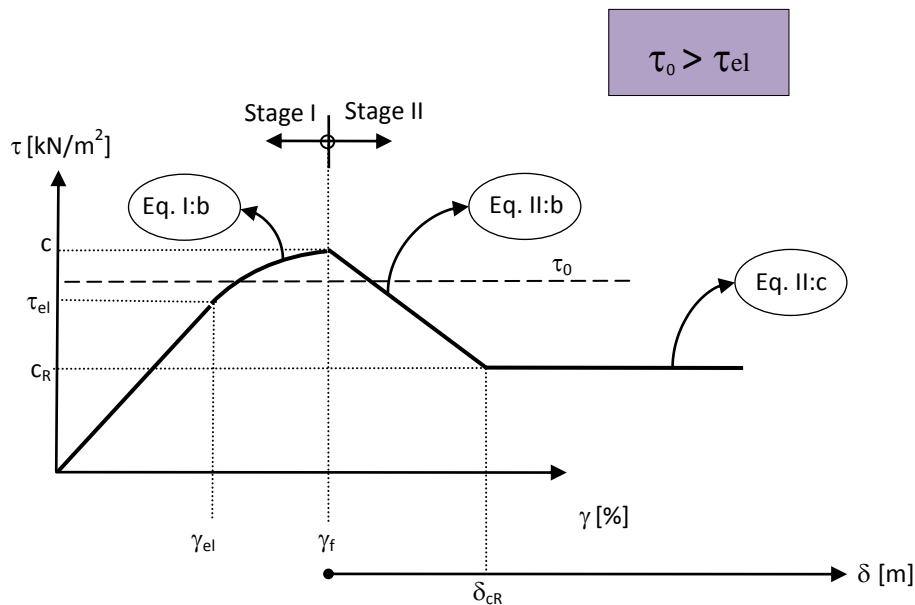


Figure 4.7. Stress-strain relationship and equations for deformation by additional stress when in situ stress exceeds the elastic limit.

If the in situ shear stress is within the linear segment of the stress-strain relationship, i.e. $\tau_0 < \tau_{el}$, the additional stress is thus calculated according to:

$$(14) \quad \text{Eq. I:a}_{el} \quad \gamma(\tau) = ((\tau + \Delta\tau_{(z)}) - \tau_{0(z)}) * \frac{\gamma_{el}}{\tau_{el(z)}}$$

If the in situ value is within the linear segment and the additional stress is between the elastic limit and the peak, i.e. $\tau_{el} < (\tau + \Delta\tau) < c$, the deformation is calculated according to:

(15) Eq. I:a

$$\delta(\tau) = \frac{\tau_{el(z)} - \tau_{0(z)}}{\tau_{el(z)}} * \gamma_{el} + (\gamma_f - \gamma_{el}) * \left(1 - \sqrt{1 - \frac{(\tau + \Delta\tau(z)) - \tau_{el(z)}}{c(z) - \tau_{el(z)}}} \right)$$

If the in situ stress exceeds the linear limit, i.e. $\tau_0 > \tau_{el}$, the following equation is used as long as the peak is not reached:

(16) Eq. I:b

$$\delta(\tau) = (\gamma_f - \gamma_{el}) * \left(1 - \sqrt{1 - \frac{\tau_{0(z)} - \tau_{el(z)}}{c(z) - \tau_{el(z)}}} - \sqrt{1 - \frac{(\tau + \Delta\tau(z)) - \tau_{el(z)}}{c(z) - \tau_{el(z)}}} \right)$$

Step by step, as the shear pressure increase, $\Delta\tau + \tau$ reach the peak value c where the slip surface forms and Stage II begins. The amount of pressure in the profile at this point, denoted τ_{max} , is the reference point when further deformation develops. From this point and on the shear strength diminish and the deformations due to the additional shear pressure, $\delta(\tau)$, is calculated according to Figure 4.8.

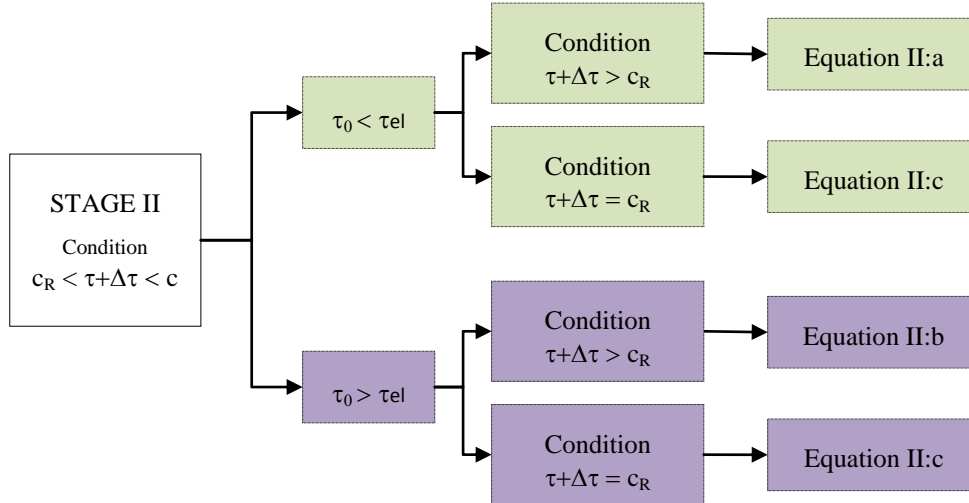


Figure 4.8. Conditions for equations in Stage II.

Deformation in the interval between the peak and the residual value, i.e.

$c_{u(z)} < (\tau + \Delta\tau(z)) < c_R$ can, if the in situ stress was within the elastic segment be calculated according to:

(17) Eq. II:a

$$\delta(\tau) = (\tau_{max(z)} - \tau_{0(z)}) * \frac{\gamma_{el}}{\tau_{el(z)}} + (\gamma_f - \gamma_{el}) * \left(1 - \sqrt{1 - \frac{\tau_{max(z)} - \tau_{el(z)}}{c(z) - \tau_{el(z)}}} \right) + ((\tau + \Delta\tau(z)) - \tau_{max(z)}) * \frac{\gamma_{el}}{\tau_{el(z)}}$$

If the in situ stress exceeded the elastic limit for the same interval, the deformation post-peak can be calculated as:

$$(18) \quad \text{Eq. II:b} \quad \delta(\tau) = (\gamma_f - \gamma_{el}) * \left(\sqrt{1 - \frac{\tau_0(z) - \tau_{el}(z)}{c_{u(z)} - \tau_{el}(z)}} - \sqrt{1 - \frac{\tau_{\max}(z) - \tau_{el}(z)}{c_{u(z)} - \tau_{el}(z)}} \right) - (\tau_{\max}(z) - (\tau + \Delta\tau_{(z)})) * \frac{\gamma_{el}}{\tau_{el}(z)}$$

The decrease of shear strength continues until it reaches the in situ value. The entire load bearing capacity will then be used and the maximal force N_{crit} corresponds with the critical load that can be applied. The additional load per square meter that can be placed on the surface of the slope is then calculated as previously mentioned by dividing the maximal horizontal force with the depth to the slip surface.

In order to determine the amount of displacement, denoted δ_{instab} , that the slope can be subjected to momentarily, the pressure is reduced further until it reaches the residual value. This corresponds for example with a scenario with extensive piling which imposes displacement of the soil. As the deformation thus continues, the residual shear strength is reached and at this level, the deformation due to shear strength is calculated as before but with an addition:

$$(19) \quad \text{Eq. II:c} \quad \delta(\tau) = \text{eq. II: a or II: b} - (\tau_{\max}(z) - c_R) * \frac{\gamma_{el}}{\tau_{el}(z)}$$

The displacement when the residual strength is reached depends only on the force N . A slip deformation is thus added at the slip surface to regulate the difference between the shear stress deformation and the displacement caused by the horizontal pressure. This assumption is made only at the slip surface and not the other depths, so this addition is made together with the summation of deformation for the calculation step.

A complete list of equations used in the Excel sheet can be found in Appendix 1.

4.2.1 Verification with previous examples by Bernander

Since the spreadsheet used in this thesis is an attempt to simplify earlier versions by Stig Bernander, comparisons with previous results are made to assess the reliability of the calculations. The principal difference likely to affect the outcome, regards the partitioning of the slope. This has previously been done by regulation of the shear pressure addition, $\Delta\tau$, manually. In the new version, the number of calculation steps has been fixed and the intervals for the shear pressure are regulated in order to divide the spacing so that the length distance decreases closer to the peak value. As it is a finite difference problem, the number of intervals and partitioning can have an impact on the results. The effects of increasing or decreasing the number of calculation steps or changing the intervals will be examined further in the basic sensitivity analysis in a following section.

The results from calculations made with the same input data as an example calculated by Bernander (2011, pp. 193-204) show a discrepancy up to 4 percent. Figure 4.9 show the variation of five of the calculated parameters. The force, N , and distance, x , where the peak strength is reached, show little or no variation. These parameters are included in the comparison to give an indication halfway through the calculations where the shift from Stage I to II takes place. It is the outcome of the critical load that differ the most in the comparison with results from Bernander 2011 (pp. 193-204). The major contributors to the difference in results are most likely the change of calculation steps and intervals. Some part of the discrepancy can however be

accounted for by the fact that the relation between the peak strength and elastic stress values does not vary depending on depth as it ought to in Stage II of Bernander's calculations. The input to the analysis is compiled in Appendix 3 together with a table of results.

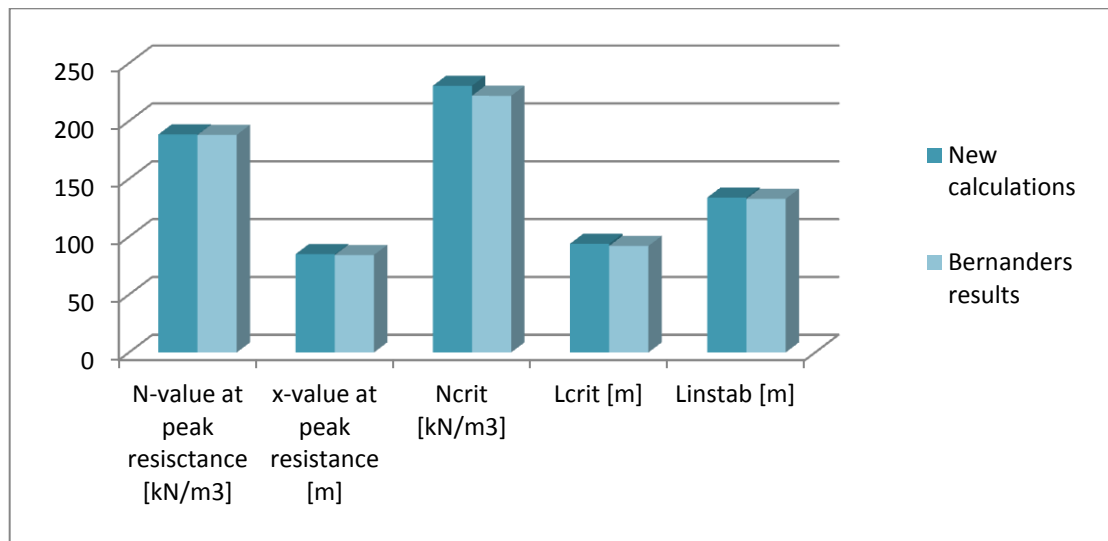


Figure 4.9. Verification with Bernander's example from 2011.

Another comparison, between the current spreadsheet and prior versions by Bernander (2008, pp. 79-100) show a relatively large variation in the critical length. The results from this comparison with the results of the Excel calculations in Appendix C of Bernander's Research Report from 2008 are presented in Figure 4.10. The input data and the results table are compiled in Appendix 3. The slope modelled in this example has a low gradient, only 1:100, and the in situ stress is as a result of this, so low that the residual strength exceeds it. For this reason the parameter of the destabilisation length has not been calculated. The discrepancy between the calculations is most likely attributed to the difference in intervals. As the difference in stress and length for each step are adjusted according to the original, the difference becomes negligible. This indicates that there can be a possible gain in increasing the number of steps in order to get more precision in the results.

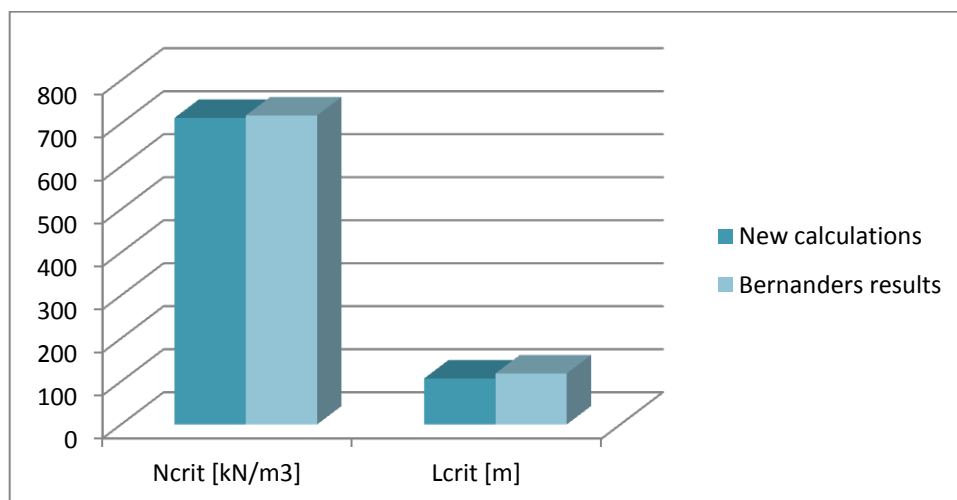


Figure 4.10. Comparison with results from Bernander published in 2008 (p.87)

The Research Report published by Bernander in 2008 also contains a sensitivity analysis with calculations performed with the two spreadsheets. A comparison of results carried out for 12 of the 16 cases presented by Bernander, is presented in Tables 4.11 to 4.15. Case 9, 10, 13 and 14 were not compared since the in situ stress is less than the residual strength, which is a condition for calculation in the new spreadsheet.

Comparisons half way through the calculations with the parameters of load capacity, N , and length, x , show a low variation of results. The calculated load, as illustrated in Figure 4.11, varies from 0 to 4 percent, with an average difference of 2 percent. The length parameter at this point, illustrated in Figure 4.12, varies slightly more, from 0 to 7 percent with an average of 4 percent.

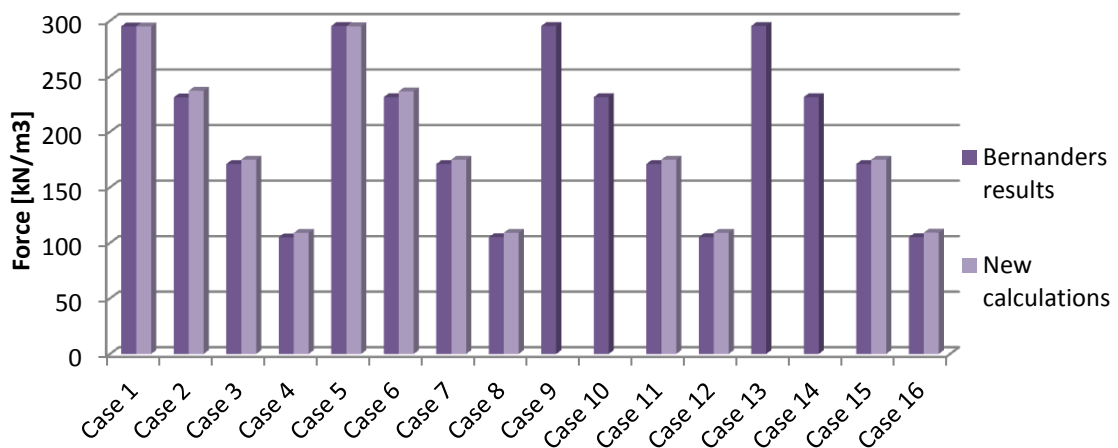


Figure 4.11. Comparison of results from 2008 for the load at the point where Stage I is at an end.

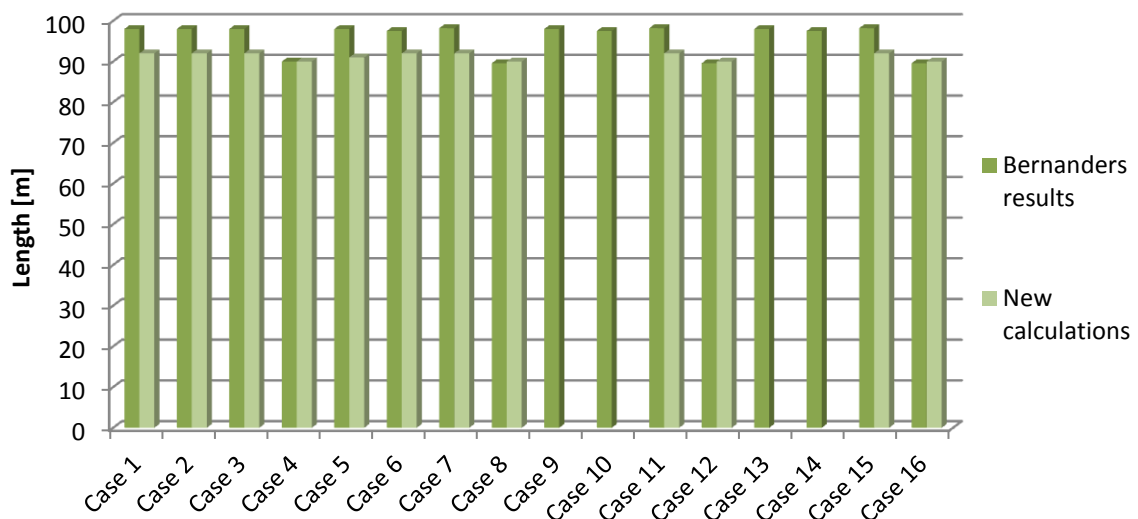


Figure 4.12. Comparison with results from 2008 of length where Stage I is at an end.

The final results of load capacity calculated for 14 of the 16 cases from 2008 show little or no discrepancy. As seen in Figure 4.13, only two of the cases vary from Bernander's results, with 3 and 4 percent respectively. The results for the deformation follow this example with little or no variation. Figure 4.14 illustrates the difference in results for the calculated influence length for the added load. This parameter show a variation that range from 0 to 6 percent and an average of 4 percent. The difference from Stage I thus continue to Stage II for this parameter.

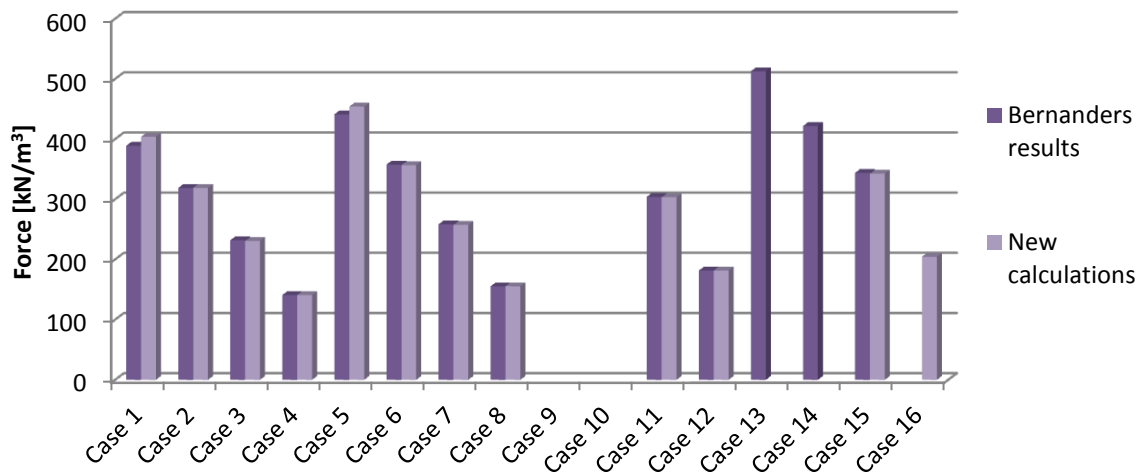


Figure 4.13. Comparison with results from 2008 of the critical force N.

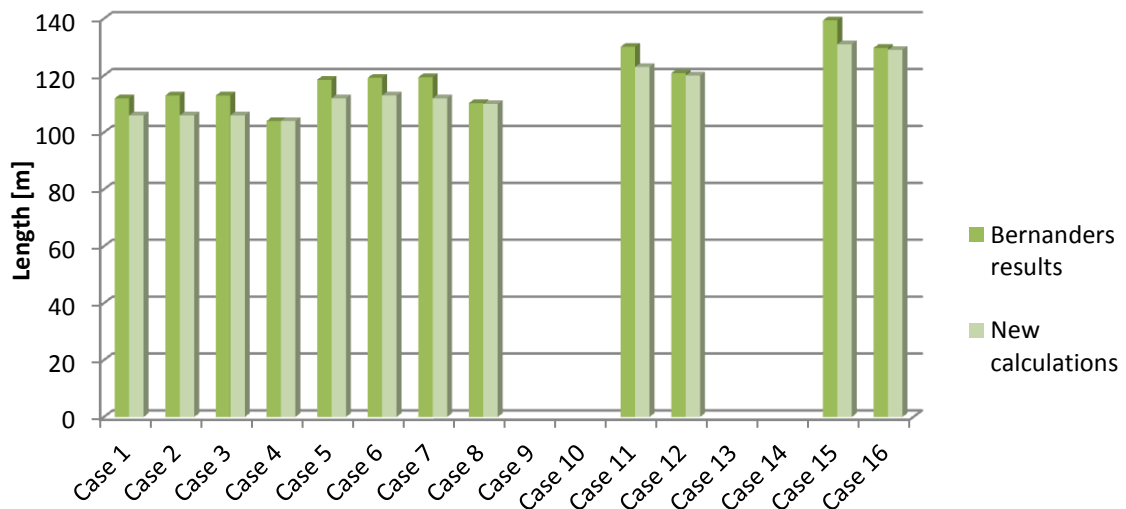


Figure 4.14. Comparison with results from 2008 of the critical length.

The calculations of influence length due to instantaneous load or deformation, L_{instab} , illustrated in Figure 4.15, differ more than any of the other results. The range goes from 3 to 18 percent with an average of 8 percent. This indicates that the results from this parameter might not be as reliable.

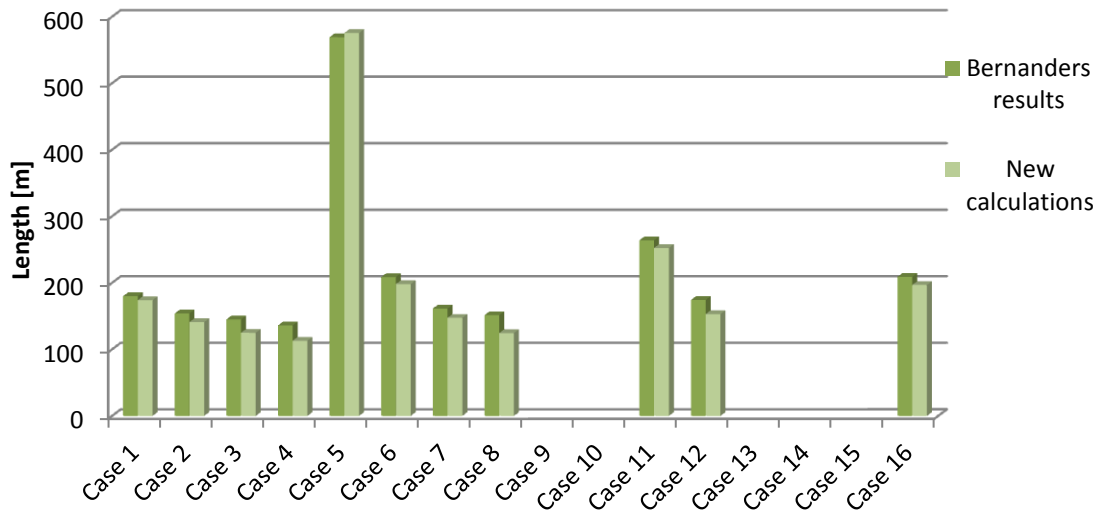


Figure 4.15 Comparison with results from 2008 of the length of influence from deformation.

4.2.2 Calculations for a new slope example

In order to perform an independent calculation and study the impact of variation of parameters, a new example of a slope is presented. The design of the slope has been kept as simple as possible in order to convey the principles of the calculation method. The depth from the surface down to the slip surface, denoted H , is set to a constant value of 20 meters. The gradient of the slope, $\Delta y/\Delta x$, is also set as a constant; in this case it is 5 percent, so that it rises 5 meter for every 100 meters in length. The shear zone is set as a third of the depth as illustrated in Figure 4.16. This is also the point of pressure for the force acting as a result of the additional load, N .

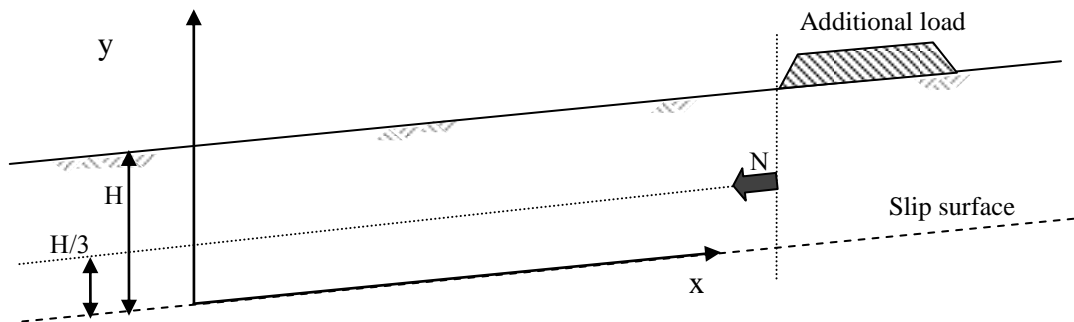


Figure 4.16. Example of a slope for spreadsheet calculations.

All the input parameters for this example slope have been compiled in Table 4.2. The elastic modulus, G , mean elastic modulus, E_{mean} , and deviator strain at elastic limit, γ_{el} , are calculated as functions of the other parameters according to the equations presented in previous section.

*Table 4.2. Input parameters to the Excel spreadsheet.
(Variables marked with * are calculated.)*

Shear strength at surface	c_s	16	kN/m ²
Peak value for shear strength evaluated in lab	c_{lab}	28	kN/m ²
Peak value for shear strength	c	31	kN/m ²
Factor for increasing or decreasing peak shear strength	c_{factor}	- 10	%
Residual value for shear strength	c_R	15	kN/m ²
Shear stress at elastic limit	τ_{el}	16	kN/m ²
Deviator strain at elastic limit *	γ_{el}	0,0105	–
Deviator strain at failure limit	γ_f	0,03	–
Elastic modulus at shear *	G	1520	–
Elastic modulus *	E_{mean}	3464	–
Poisson's ratio	ν	0,5	–
Post peak slip at $z=0$ when c_R is reached	δ_{cR}	0,2	m
Density	d_{start}	16	kN/m ²
	d_{gain}	0,1	kN/m ²
Depth to slip surface	H	20	m
Gradient	$\Delta y/\Delta x$	0,05	–
Sensitivity ratio	c_R/c	0,5	–

The peak shear strength is a product of the evaluated lab value and a chosen factor, c_{factor} , that can be used to account for uncertainties or time effects like a short or long loading time. In this case the shear strength at the surface is set to 16 kN/m² and the peak value is 28 kN/m² at the level of the slip surface. The factor for increasing or decreasing the peak shear strength is set to a 10 percent decrease in order to consider a shorter time for loading. As previously mentioned a faster loading rate will give a higher peak value and a lower residual value, as illustrated in Figure 3.3. The stress-strain relationship for this example is illustrated in Figure 4.17.

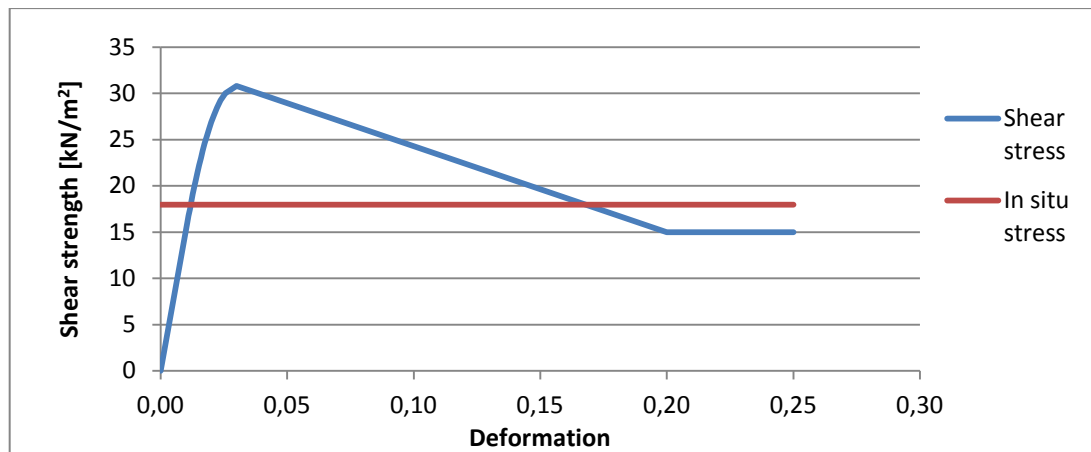


Figure 4.17 Stress-Strain relationship for the example calculation.

The stress-strain relationship has a linear dependence in the elastic phase and is then continued with a parabolic relationship to the power of 2 until the peak, just as in Bernander's calculations. An enlargement of the relationship in Stage I, until the peak shear strength, is illustrated in Figure 4.18. After the peak is reached, a linear decrease to the point of residual strength is assumed. The values for the stress-strain relationship have been chosen to resemble the input to the calculations previously performed in progressive slides by Stig Bernander which are based on empirical knowledge.

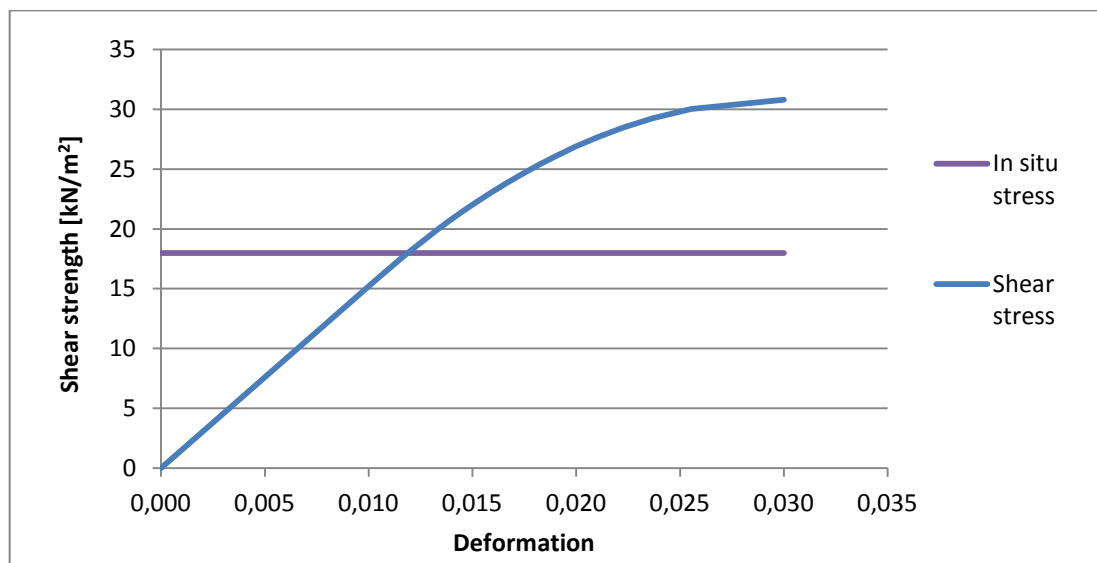


Figure 4.18 Stress-Strain relationship for Stage I in the example calculation.

A new feature in this spreadsheet is the variation of density by depth, denoted $\rho(z)$. A starting value at the surface is defined, d_{start} , and a gain, d_{gain} , is then multiplied with the distance along the z-axis according to the following equation:

$$\rho(z) = d_{start} + d_{gain} * (H - z)$$

In this example the ratio between the peak and the residual strength is 0,5. Any of the input parameters can easily be changed and the results are calculated within a few seconds with the help of Excel macro functions.

4.2.3 Calculation Results

As the input variables are entered in the spreadsheet, the critical load, length of influence and deformations can be calculated. How the shear stress and strength varies depending on depth is illustrated in Figure 4.19. The indication of depth starts at the slip surface and continues upwards.

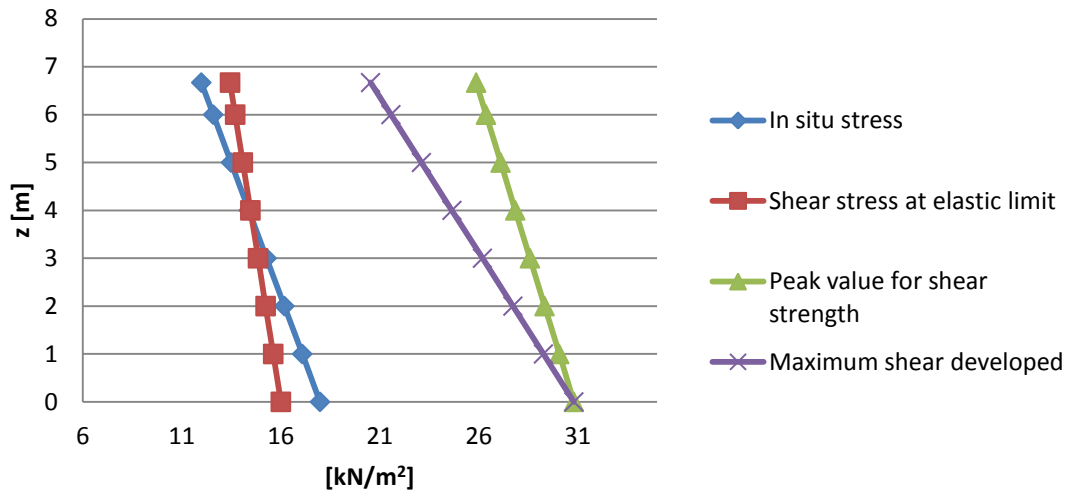


Figure 4.19. Variation of shear stress and strength in the shear zone of $H/3$ for the calculation example. z [m] indicates distance from slip surface.

For each calculation step the pressure adds up, until the peak is reached. Stage II then continues with a decline to the in situ value. The development of this parameter, $\tau + \Delta\tau$, is illustrated in Figure 4.20.

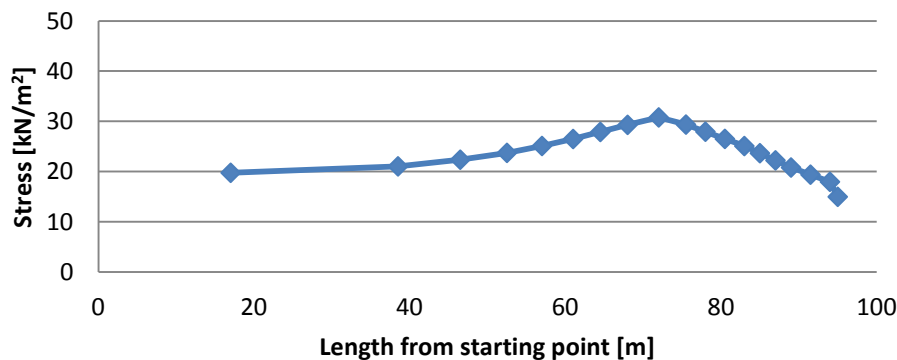


Figure 4.20. Development of shear pressure, $\tau + \Delta\tau$, in the calculated example.

Results of the calculations show that the slope in this example can suffer an additional load of 21 kN/m^2 . That corresponds with a horizontal force, N_{crit} , of about 419 kN/m^3 . The influence length, L_{crit} , of this added pressure is 114 meters, as illustrated in Figure 4.21. Beyond that, length no stabilising forces can be mobilised to counterweigh such additional long term load. The deformation at the slip surface for this scenario is also illustrated in Figure 4.21. When the in situ value is reached and all the shear capacity is used the clay is deformed about 0,19 meters. If the load is instantaneous or only in the form of enforced deformation e.g. caused by piling, the deformation is 0,61 meters. The influence length, L_{instab} , corresponding with this deformation is 141 meters. A table of all calculation results for this example is compiled in Appendix 4.

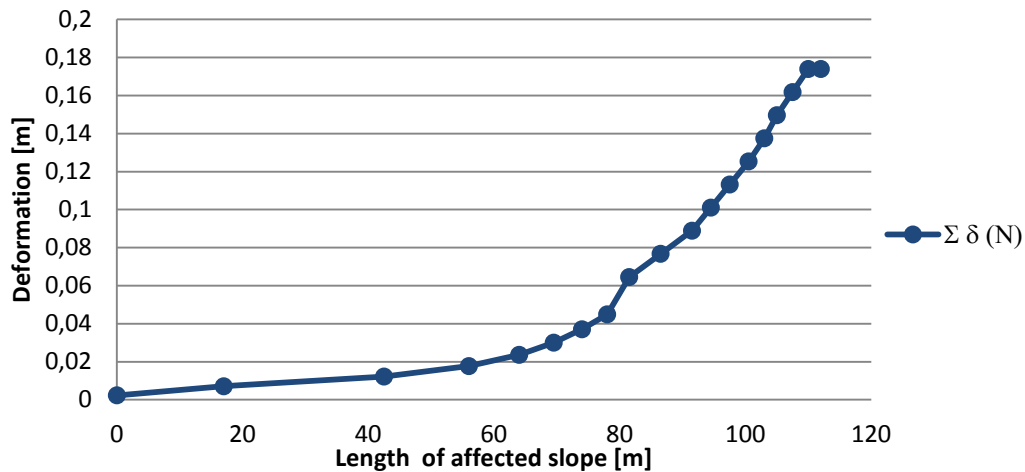


Figure 4.21. Calculated deformation and length of the affected area in the slope example.

4.2.4 Sensitivity Analysis

The outcome of a finite difference calculation can sometimes be sensitive to the partitioning or division of intervals. In this analysis it is Stage I with the curved interval from the elastic limit to the peak value that is most likely to affect the results. For Stage II with the linear decline in shear strength, the number and partitioning of intervals are not as likely to affect the outcome. A comparison of results using a total number of steps varying from 10 to 20 and 26 is illustrated in Figure 4.22. The input variables are the same as in the slope example presented above where a total of 20 steps were used.

Comparison shows that the number of calculation steps has little impact on the critical load when the number of steps is reduced. If they are increased from 20 to 26 the results for the additional load increase with 4 percent. The influence length is more affected by the number of calculation steps. Comparison between the original 20 steps, a decrease to 10 steps and an increase to 26 steps, show a variation of results from minus 7 percent to an increase of 13 percent respectively. The change of the critical deformation is negligible which indicates that this parameter might be relatively stable. A complete table of results is included in Appendix 4.

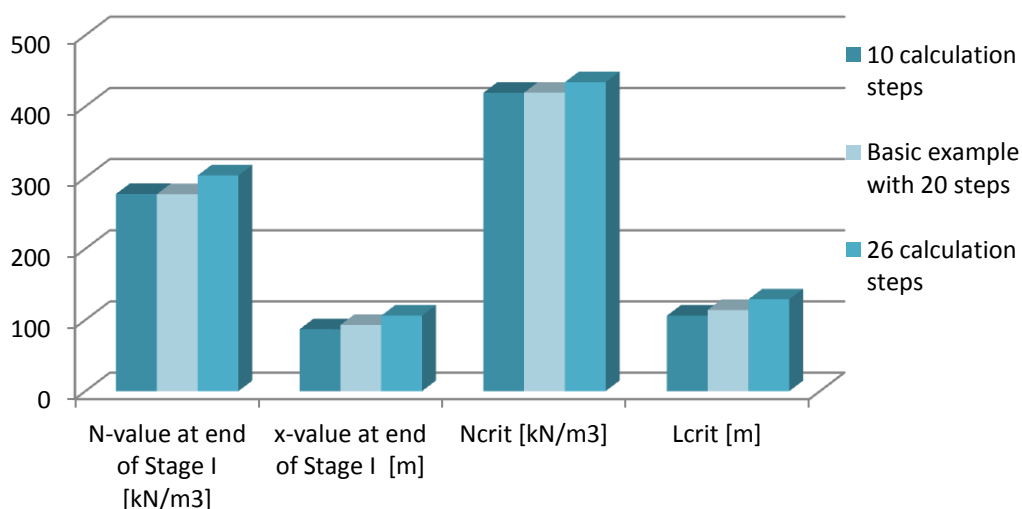


Figure 4.22. Comparison of results depending on number of calculation steps.

Results from the comparison with a reduced or increased number of calculation steps are also plotted as illustrated in Figure 4.23 for the critical load and Figure 4.24 for the critical length. The aim of further development of the model might be to find a number of calculation steps for which the curve of results can level out and become stable.

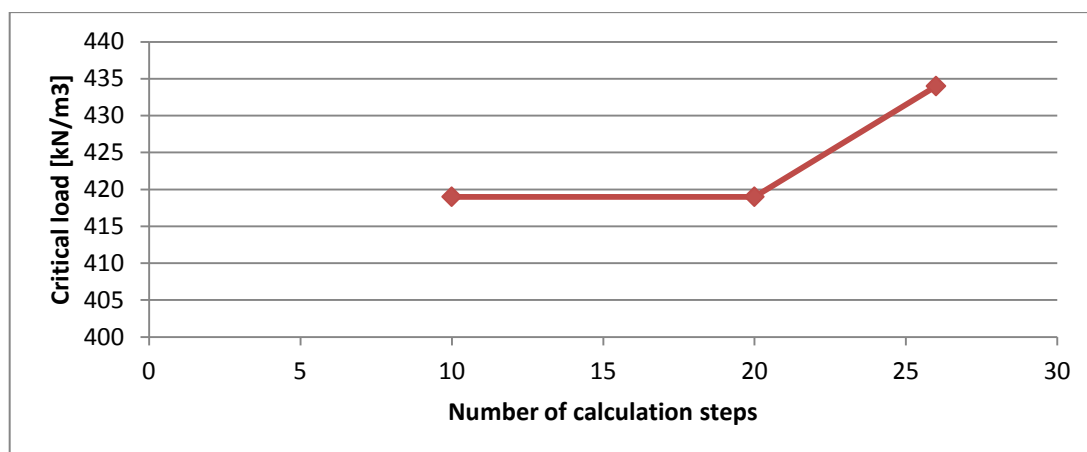


Figure 4.23. Variations of results for the critical load depending on number of calculation steps. Note that the vertical scale does not begin at zero.

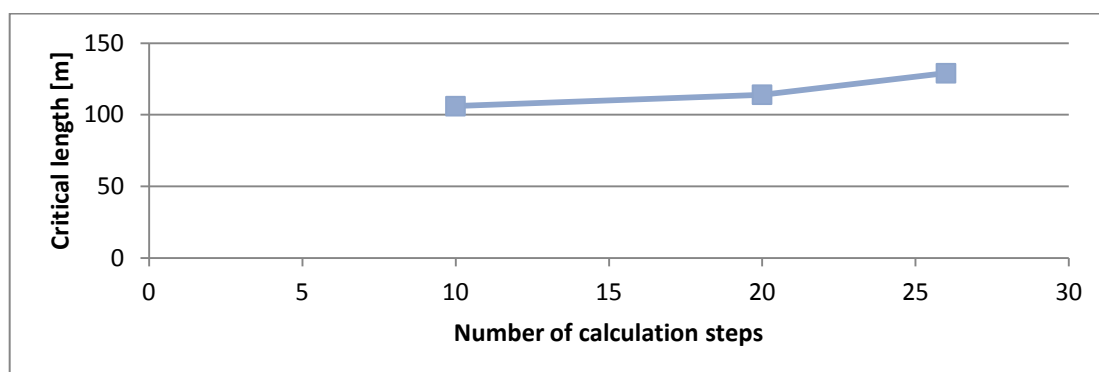


Figure 4.24. Variations of results for the critical length depending on number of calculation steps.

As mentioned before, the structure of the spreadsheet allows a simple variation of input data. A basic sensitivity analysis is presented in Figure 4.25. The figure illustrates how a change of a single variable can have a reasonably large impact on the results. All the calculation results in Figure 4.25 are normalised in order to show the relation to the basic example, illustrated with the value of 1. The effects of varying the residual strength have previously been investigated by Bernander (2008 and 2011). If the residual strength is lowered from 15 kN/m² to 10 kN/m² the load capacity decrease about 10 percent. If the residual strength is increased from 15 kN/m² to 17 kN/m² the load capacity increase by about 6 percent. Another factor that has a large impact on the results relates to the loading time. If the factor for increase of the peak shear strength is decreased by 10 percent, that leads to a decreased capacity of about 19 percent. This reduction also affects the influence length by about 3 percent.

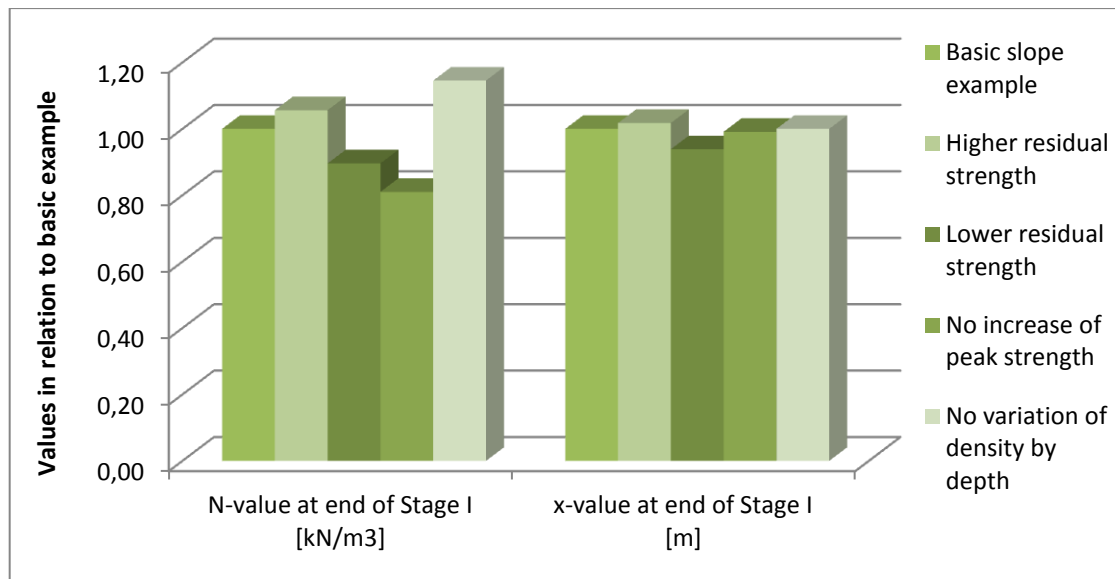


Figure 4.25. Effect on the critical load and length by variation of input. The comparison show the results in relation to the basic example.

The sensitivity analysis further reveals that the additional function in this spreadsheet with density variation by depth also can have an impact on the results. An increase of density per meter by just 0,1 kN/m² results in a decrease of the calculated additional load by 15 percent compared to the case where the density was constant, independent of depth.

The change of results in the deformation is presented in Figure 4.26. Variations in results for the calculations of the critical deformation correlate fairly well with the results of the critical load. The calculation results for the momentarily deformation caused by a short term load or forced displacement like piling reveals large differences. The conclusion in this case might be that this parameter is a bit unstable and that the impact of the variables is perhaps too high.

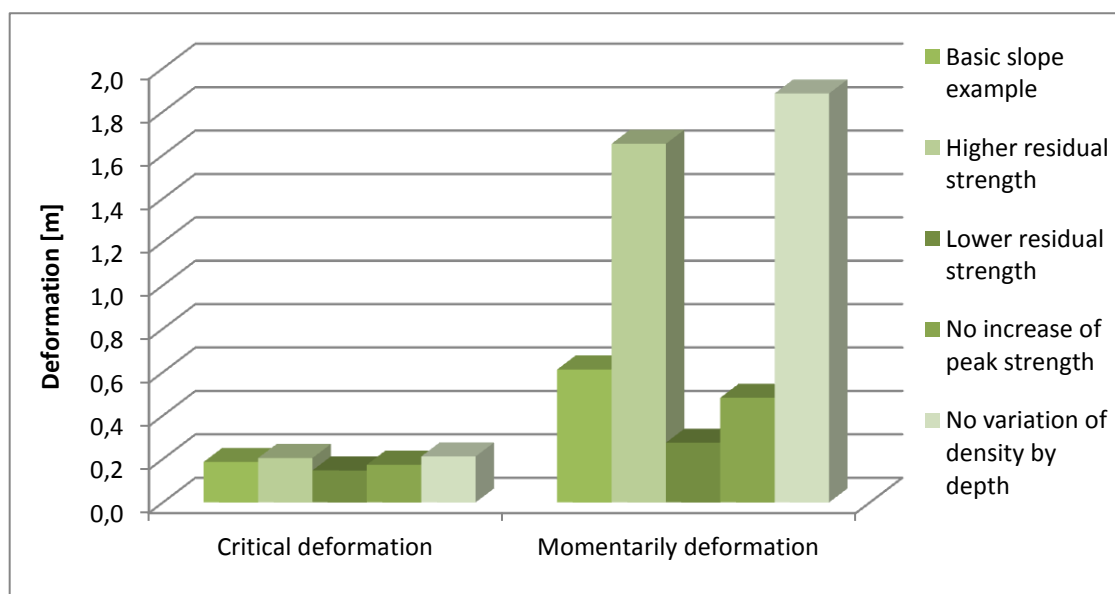


Figure 4.26. Effect on the resulting deformation by variation of input.

5 Discussion

The intension of this chapter is to discuss some of the concerns with the model and to point out the principal advantages. The results of the calculations are commented and some suggestions for future development are made. The issue of uncertainties and safety factors is also discussed.

5.1 Comments on the model and calculation method

It is important to remember that in the attempt to simplify, important aspects may be lost. One of the major constraints of the current version of this basic spreadsheet is that only slopes with a constant gradient and depth to slip surface can be modelled. This can however be addressed if the spreadsheet is developed further so that the calculation steps are taken in fixed distances according to the geometry of the slope. The Solver tool can then be used in order to find the corresponding pressure so that the compatibility criterion is fulfilled. Bernander mentions this possibility along with other suggested developments (Bernander, 2011). The analysis method can also be applicable to retrogressive or lateral slides as investigated in connection with landslides in e.g. Canada (Locat, 2007).

It may be noted that in the case of forced deformations as in piling, the influence of added pore pressure is also very likely to affect the outcome (Bernander, 2008, p. 25). This aspect is not included in the original spreadsheet calculations and no addition on this point has been made in the new version.

Another drawback of the method can be that the engineer has to make a preliminary judgement about the location of the potential slip surface. The short calculation time can however allow a series of calculations to be performed, thus mitigating this disadvantage. The easy variation of parameters allows for a statistical analysis with determination of confidence intervals for the results.

Microsoft Excel is a software that most engineers have at least a basic familiarity with. This fits the purpose of making the method as accessible as possible. The first priority in designing the spreadsheet has been to make the computations easy to perform. The intension has also been to make the calculation process as transparent as possible in order to convey the principles of the method. The ideal is that a user should be able to get quick and easy results without compromising the ability to judge the reliability and constraints of the calculations.

The sensitivity analysis revealed some discrepancy between the results from Bernander's calculations and the ones performed within this study. The parameters connected with the instantaneous load or forced deformation, denoted N_{instab} , L_{instab} and δ_{instab} , deviated most. This indicates that the results of the new calculations for these parameters may be less reliable and should be reviewed. The discrepancy for the other variables was within a tolerable margin. The most likely cause of the deviation in this case, is the number of calculation steps and intervals for the added pressure. This issue was investigated for the new spreadsheet version and the increase of steps from 20 to 26 gave an increase of the critical length by 13 percent. The calculation of the critical load varied less and the deformation was almost the same. This indicates that the calculation of deformations might be associated with less uncertainty.

In order to address the issue of strain-softening, reliable input to the analysis require more research as to the behaviour of clay after the peak shear strength is reached. The variables used in the analysis today, are based on empirical values implemented by

Bernander in his application of the model. Although the relationship is a significant component in the analysis method, Bernander clearly points out that the most important part of the progressive failure analysis is that of taking deformation within the sliding soil mass in consideration (Bernander, 2008, p. 44).

5.2 Discussion of relevant safety factors

Calculations can sometimes seem deceptive in the sense that they yield a definite number with many decimals. This precision does not however, equal reliability. The basic sensitivity analysis showed a relatively large variation in results just by changing a single parameter. Safety factors are crucial in reducing the effects of simplifications and uncertainties.

The current use of a quota between the average and mobilised shear strength does not apply to this model. The available shear resistance varies as a consequence of applying the deformation-softening concept. The relevancy of a fixed average value for the shear resistance can thus contradict the purpose of the method. Instead, a ratio between the calculated critical load effect and the load effect from the planned measure that might cause interference is suggested for this type of brittle system where the residual strength is less than the in situ stress (Bernander, 2011, pp. 34-35).

Factor of safety:
$$F = \frac{N_{crit}}{N_{disturbance}} > 1$$

The safety factor can also be calculated as a relationship between the critical deformation and the calculated deformation caused by the applied disturbance. In that way the safety factor becomes more comprehensible and not just a concept that cannot be measured:

Alternative factor of safety:
$$F = \frac{\delta_{crit}}{\delta_{disturbance}} > 1$$

The value of the safety factor should be based upon an assessment of both risks and consequences. An extensive in-depth analysis may require a lower safety factor. Likewise, if the affected area involves little or no consequences for human or natural life, a lower safety factor may be admitted.

6 Conclusions

The concept of progressive failure enables consideration of deformations formed in the shear zone of the slope. Allowing also for influence from the deformation-softening properties of soft Scandinavian clay, the method of analysis as developed by Stig Bernander may be able to explain characteristics of some of the large landslides in Sweden. Using finite difference calculations in Excel enable a quick risk evaluation. The model allows for an easy variation of parameters that can be useful when performing a statistical analysis. The spreadsheet offers an introduction to the analysis method and allows for many possible adaptations and potential developments. An adjustment of the model in regard to the slope geometry is one of the most important areas for future development. A better determination of the deformation softening parameters is also recommended in order to improve the reliability of the model.

Within the performed sensitivity analysis, a comparison of results showed that altering the number of calculation steps and intervals had an impact on both the critical length and calculated additional load. The parameter of deformations showed less of this variation.

A relevant safety factor for calculations based on this model can be determined as a quota between the critical deformation and the deformation caused by the disturbance. The deformation can be relatively easily measured and a safety factor based on this variable has the additional advantage of making the concept of a safety factor more comprehensible.

7 References

- Andresen, L. (2002). *Capacity Analysis of Anisotropic and Strain-Softening Clay*. Oslo: University of Oslo.
- Bernander, S. (2008). *Down-hill Progressive Landslides in Soft Clays. Triggering Disturbance Agents. Slide Propagation over Horizontal or Gently Sloping Ground. Sensitivity Related to Geometry*. Luleå: Luleå University of Technology.
- Bernander, S. (2000). *Progressive Landslides in Long Natural Slopes. Formation, potential extension and configuration of finished slides in strain-softening soil. Licentiate Thesis*. Luleå: Luleå University of Technology.
- Bernander, S. (2011). *Progressive Landslides in Long Natural Slopes. Formation, Potential Extension and Configuration of Finished Slides in Strain-Softening Soils*. Luleå: Luleå University of Technology.
- GEO-SLOPE International Ltd. (2008). *Stability Modeling with SLOPE/W 2007 Version. An Engineering Methodology*. Calgary, Alberta, Canada: GEO-SLOPE International Ltd.
- Gylland, A. S., Nordal, S., Jostad, H. P., & Mehli, M. (2011). Pragmatic Approach for Estimation of Slope Capacity in Soft Sensitive Clay. *EJGE*, 575-590.
- Implementeringskommissionen för Europastandarder inom Geoteknik. (2010). *IEG Rapport 4:2010. Tillståndbedömning/klassificering av naturliga slänter och slänter med befintlig bebyggelse och anläggningar*. Stockholm: IEG.
- Lacasse, S., Berre, T., & Lefebvre, G. (1985). *Block sampling of Sensitive Clays*. San Francisco: Proc. of 11th International Conference on Soil Mechanics and Foundation Engineering.
- Larsson, R. (2008). *Information 1. Jordens egenskaper*. Linköping: Swedish Geotechnical Institute.
- Larsson, R., Ottosson, E., & Sällfors, G. (1997). *SIG Report no 44. Agnesbergsskredet*. Linköping: Swedish Geotechnical Institute.
- Locat, A. (2007). *Étude d'un étalement latéral dans les argiles de l'Est du Canada et de la rupture progressive, Le cas du glissement de Saint-Barnabé-Nord*. Québec: Université Laval.
- Royal Swedish Academy of Engineering Sciences: Commission on Slope Stability. (1995). *Papport 3:95. Anvisningar för släntstabilitetsutredningar*. Linköping: IVA Skredkommissionen.
- Sällfors, G. (1994). *Slänters Stabilitet*. Göteborg: Chalmers University of Technology.
- Swedish Geotechnical Institute. (2012). *Varför inträffar skred?* Retrieved July 3, 2012, from Swedish Geotechnical Institute: www.swedgeo.se
- Yu, H. S., Salgado, R., Sloan, S., & Kim, J. (1998). Limit Analysis versus Limit Equilibrium for Slope Stability. *ASCE. Journal of Geotechnical and Geoenvironmental Engineering*, 1-10.

Appendix 1. Compilation of equations in Excel

Elastic modulus $E_{mean} = \frac{G}{c} * 2 * (1 + \nu) \frac{(c_s * c)}{2}$

Deviator stain at el limit $\gamma_{el} = \frac{\gamma_f * \tau_{el}}{(2 * c - \tau_{el})}$

Shear modulus $G = \frac{\tau_{el}}{\gamma_{el}}$

Peak value for shear strength $c = increase\ factor * c_{lab}$

In situ conditions:

Shear stress $\tau_{0(z=0)} = \rho(z) * H * \sin(\arctan(grad))$

$$\tau_{0(z=n)} = \tau_{0(z=0)} * \left(\frac{1 - \Delta Z}{H} \right)$$

Shear strength $c(z) = c - \frac{c - c_s}{H} * z$

Stress at elastic limit $\tau_{el(z)} = \tau_{el} * \frac{c(z)}{c}$

Density $\rho(z) = d_{start} + d_{gain} * (H - z)$

For each Δx -section

Shear stress $\tau_{(z=0)} = \tau_o(z = 0)$

$$\tau_{(z)} = \tau_{(z=0)} * \left(\frac{1 - \Delta Z}{H} \right)$$

Additional shear stress $\Delta\tau_{(z=0)} = input, example\ 0.3, 1, 2, 3 \dots$

$$\Delta\tau_{(z)} = \Delta\tau_{(z=0)} * \left(\frac{1 - \Delta Z}{H} \right)$$

Resulting shear stress $(\tau + \Delta\tau_{(z)}) = \tau_{(z)} + \Delta\tau_{(z)}$

Deformation, if $\tau + \Delta\tau_{(z)} < \tau_{el(z)}$ then:

(Eq. I:a_{el}) $(\tau) = ((\tau + \Delta\tau_{(z)}) - \tau_{0(z)}) * \frac{\gamma_{el}}{\tau_{el(z)}}$

Deformation, if $\tau_{0(z)} < (\tau + \Delta\tau_{(z)}) < c(z)$ and $\tau_{0(z)} > \tau_{el(z)}$ then:

(Eq. I:b) $\delta(\tau) = (\gamma_f - \gamma_{el}) * \left(1 - \sqrt{1 - \frac{\tau_{0(z)} - \tau_{el(z)}}{c(z) - \tau_{el(z)}}} - \sqrt{1 - \frac{(\tau + \Delta\tau_{(z)}) - \tau_{el(z)}}{c(z) - \tau_{el(z)}}} \right)$

Deformation, if $\tau_{0(z)} < (\tau + \Delta\tau_{(z)}) < c(z)$ and $\tau_{0(z)} < \tau_{el(z)}$ then:

(Eq. I:a) $\delta(\tau) = \frac{\tau_{el(z)} - \tau_{0(z)}}{\tau_{el(z)}} * \gamma_{el} + (\gamma_f - \gamma_{el}) * \left(1 - \right.$

$$\left. 1 - \frac{(\tau + \Delta\tau_{(z)}) - \tau_{el(z)}}{c(z) - \tau_{el(z)}} \right)$$

Deformation, if $c(z) < (\tau + \Delta\tau_{(z)}) < c_R$ and $\tau_{0(z)} > \tau_{el(z)}$ then:

$$\text{(Eq. II:b)} \quad \delta(\tau) = (\gamma_f - \gamma_{el}) * \left(\sqrt{1 - \frac{\tau_{0(z)} - \tau_{el(z)}}{c(z) - \tau_{el(z)}}} - \sqrt{1 - \frac{\tau_{\max(z)} - \tau_{el(z)}}{c(z) - \tau_{el(z)}}} \right) - (\tau_{\max(z)} - (\tau + \Delta\tau_{(z)})) * \frac{\gamma_{el}}{\tau_{el(z)}}$$

Deformation, if $c(z) < (\tau + \Delta\tau_{(z)}) < c_R$ and $\tau_{0(z)} < \tau_{el(z)}$ then:

(Eq. II:a)

$$\delta(\tau) = (\tau_{\max(z)} - \tau_{0(z)}) * \frac{\gamma_{el}}{\tau_{el(z)}} + (\gamma_f - \gamma_{el}) * \left(1 - \sqrt{1 - \frac{\tau_{\max(z)} - \tau_{el(z)}}{c(z) - \tau_{el(z)}}} \right) + ((\tau + \Delta\tau_{(z)}) - \tau_{\max(z)}) * \frac{\gamma_{el}}{\tau_{el(z)}}$$

Deformation, if $\tau + \Delta\tau_{(z)} = c_R$ and $z = 0$ then:

$$\text{(Eq. II:c)} \quad \delta(\tau) = \text{Eq. II: b or II: a} - (\tau_{\max(z)} - c_R) * \frac{\gamma_{el}}{\tau_{el(z)}}$$

Deformation, if $\tau + \Delta\tau_{(z)} > c_R$ then:

$$\delta(x) = \delta_{cR} * (c - (\tau + \Delta\tau) / (c - c_R))$$

$$\text{Additional earth pressure} \quad \Delta N = \left(\frac{(\tau + \Delta\tau_{(z=0)} + \tau_{(z=0)})}{2} - \tau_{0(z=0)} \right) * \Delta x$$

$$\text{Sum of added earth pressure} \quad \Sigma \Delta N_{(x=n+1)} = \left(\frac{(\tau + \Delta\tau_{(z=0)} + \tau_{(z=0)})}{2} - \tau_{0(z=0)} \right) * \Delta x + \Delta N_{(x=n)}$$

$$\text{Sum of displacement} \quad \Sigma \delta(N) = \frac{(\Delta N_{(x=n)} + \Delta N_{(x=n+1)})}{2} * \frac{\Delta x}{E_{\text{mean}} * H}$$

$$\text{Compatibility criterion} \quad C = \Sigma \delta(N) - \Sigma \delta(\tau)$$

$$\text{Surface load} \quad q = \frac{N_{\text{crit}}}{H}$$

Appendix 2. Translation of Equation numbering

The numbering of equations in this thesis does not correspond to the numbering in previous literature on the topic written by Stig Bernander.

In order to be able to follow the derivation of the equations, a translation is helpful:

Table 1. Translation of equation numbering.

Equation number in this thesis	Equation number in Bernander's litterature
I:a _{el}	I:1
I:a	I:4a
I:b	I:4
II:a	I:5a
II:b	I:5
II:c	I:5b

Appendix 3. Input and results from verifications with previous versions of spreadsheets developed by Bernander

Input to the calculations for a comparison with the results by Bernander in 2011, pp. 193-204 are presented in Table 1:

Table 1. Input to comparison with calculation results from 2011.

Shear strength at surface	c_s	15	kN/m ²
Peak value for shear strength evaluated in lab	c_{lab}	30	kN/m ²
Peak value for shear strength	c	30	kN/m ²
Residual value for shear strength	c_R	15	kN/m ²
Shear stress at elastic limit	τ_{el}	20	kN/m ²
Deviator strain at elastic limit	γ_{el}	0,0375	%
Deviator strain at failure limit	γ_f	0,075	%
Elastic modulus at shear	G	533	-
Elastic modulus	E_{mean}	1200	-
Poisson's ratio	ν	0,5	-
Post peak slip at $z=0$ when c_R is reached	δ_{cR}	0,3	m
Density:	d_{start}	16	kN/m ³
	d_{gain}	0	kN/m ³
Depth to slip surface	H	20	m
Gradient	$\Delta y/\Delta x$	0,0652	-
Sensitivity ratio	c_R/c_u	0,5	-

The results from the verification with the example published by Bernander in 2011 is presented in Table 2.

Table 2. Results from comparison with example by Bernander 2011.

2011				
Explanation	Denotation	Results from new calculations	Bernander's results	Difference
Change where stage I-II	N-value	188	188	0%
Change where stage I-II	x-value	85	84	-1%
Critical Load	N_{crit}	230	222	-4%
Critical length	L_{crit}	94	92	-2%
	L_{instab}	134	133	-1%

The following input parameters in Table 3, are used in the calculation for the example by Bernander in 2008, pp.79-100.

Table 3. Input to comparison with calculation results from 2008.

Shear strength at surface	c_s	18	kN/m ²
Peak value for shear strength evaluated in lab	c_{lab}	30	kN/m ²
Peak value for shear strength	c	30	kN/m ²
Residual value for shear strength	c_R	10	kN/m ²
Shear stress at elastic limit	τ_{el}	18	kN/m ²
Deviator strain at elastic limit	γ_{el}	0,0129	%
Deviator strain at failure limit	γ_f	0,03	%
Elastic modulus at shear	G	1400	-
Elastic modulus	E_{mean}	3360	-
Poisson's ratio	ν	0,5	-
Post peak slip at $z=0$ when c_R is reached	δ_{cR}	0,2	m
Density	d_{start}	16	kN/m ³
	d_{gain}	0	kN/m ³
Depth to slip surface	H	20	m
Gradient	$\Delta y/\Delta x$	0,01	-
Sensitivity ratio	c_R/c_u	0,3	-

Table 4 contains the calculation results for the comparison with the example in Appendix C of Bernander's Research Report published in 2008.

Table 4. Comparison with previously published example by Bernander 2008.

2008				
Explanation	Denotation	Results from new calculations	Bernander's results	Difference
Critical Load	N_{crit}	713	719	1%
Critical length	L_{crit}	107	119	10%

The input variables and results from the comparison with the results from the 16 cases in Bernander's publication in 2008 is presented in Table 5.

Table 5. Comparison with previously published examples in sensitivity analysis by Bernander 2008.

2008	Input variables		Bernander's results								New calculations							
Case	c_R	Grad	N where Stage I ends	x where Stage I ends	N_{crit}	L_{crit}	L_{instab}	δ where Stage I ends	δ_{crit}	δ_{instab}	N where Stage I ends	x where Stage I ends	N_{crit}	L_{crit}	L_{instab}	δ where Stage I ends	δ_{crit}	δ_{instab}
1	10	0,05	295	98	389	112	180	0,081	0,156	0,366	295	92	404	106	174	0,081	0,164	0,371
2	10	0,06	231	98	319	113	154	0,065	0,132	0,243	237	92	319	106	141	0,068	0,132	0,216
3	10	0,07	171	98	232	113	145	0,051	0,098	0,168	175	92	231	106	125	0,053	0,098	0,131
4	10	0,08	105	90	141	104	136	0,034	0,062	0,105	109	90	141	104	113	0,036	0,062	0,072
5	15	0,05	295	98	441	119	569	0,081	0,203		295	91	454	112	576	0,081	0,210	
6	15	0,06	231	98	358	119	209	0,065	0,168	0,42	237	92	357	113	198	0,068	0,168	0,400
7	15	0,07	171	98	258	119	161	0,051	0,124	0,224	175	92	258	112	147	0,053	0,124	0,192
8	15	0,08	105	90	156	110	151	0,034	0,077	0,135	109	90	156	110	125	0,036	0,077	0,095
9	20	0,05	295	98				0,081	0,232									
10	20	0,06	231	98				0,065	0,227									
11	20	0,07	171	98	304	130	264	0,051	0,175	0,492	175	92	303	123	252	0,053	0,175	0,472

2008	Input variables		Bernander's results								New calculations							
Case	c_R	Grad	N where Stage I ends	x where Stage I ends	N_{crit}	L_{crit}	L_{instab}	δ where Stage I ends	δ_{crit}	δ_{instab}	N where Stage I ends	x where Stage I ends	N_{crit}	L_{crit}	L_{instab}	δ where Stage I ends	δ_{crit}	δ_{instab}
12	20	0,08	105	90	182	121	174	0,034	0,107	0,196	109	90	182	120	153	0,036	0,107	0,152
13	22,5	0,05	295	98	513			0,081										
14	22,5	0,06	231	98	422			0,065										
15	22,5	0,07	171	98	344	139		0,051	0,226		175	92	343	131		0,053	0,221	
16	22,5	0,08	105	90	205	130	209	0,034	0,137	0,276	109	90	205	129	197	0,036	0,137	0,242

2008	Difference							
	N where Stage I ends	x where Stage I ends	N_{crit}	L_{crit}	L_{instab}	δ where Stage I ends	δ_{crit}	δ_{instab}
Case 1	0%	-6%	4%	-5%	-3%	0%	5%	1%
Case 2	3%	-6%	0%	-6%	-8%	4%	0%	-11%
Case 3	2%	-6%	0%	-6%	-14%	4%	0%	-22%
Case 4	4%	0%	0%	0%	-17%	5%	0%	-31%
Case 5	0%	-7%	3%	-5%	1%	0%	4%	
Case 6	2%	-6%	0%	-5%	-5%	4%	0%	-5%
Case 7	2%	-6%	0%	-6%	-9%	4%	0%	-14%
Case 8	4%	0%	0%	0%	-18%	5%	0%	-30%
Case 11	2%	-6%	0%		-5%	4%	0%	-4%
Case 12						5%	0%	-22%
Case 15	2%	-6%	0%		-6%	4%	-2%	
Case 16	4%	0%	0%		-1%	5%	0%	-12%
<i>Average Difference</i>	2%	-4%	0%		-4%	4%	1%	-15%

Appendix 4. Results from Sensitivity analysis

Table 3.4. Calculation results for slope example

Parameter	Unit	With density gain by depth	Same density at all depths		No addition to the peak value		With 10 steps		With 26 steps	
			Result	Difference	Result	Difference	Result	Difference	Result	Difference
N-value	kN/m ³	277	313	13%	303	-22%	277	0%	303	9%
x-value	m	93	93	0%	106	-3%	87	6%	106	14%
N _{crit}	kN/m ³	419	480	15%	434	-19%	419	0%	434	4%
L _{crit}	m	114	114	0%	129	-1%	106	7%	129	13%
L _{instab}	m	141	490	248%	-	-19%	-	-	-	-
q	kN/m ²	21	24	15%	22	-19%	21	0%	22	5%
δ _{crit}	m	0,19	0,21	14%	0,19	-7%	0,19	0%	0,19	0%
δ _{instab}	m	0,61	1,91	212%	-	-21%	-	-	-	-